NATIONAL INSTITUTE FOR CONGESTION REDUCTION

FINAL REPORT
JUNE 2023

Transit Priority

Saeid Soleimaniamiri
Xiaopeng Li
Keke Long

National Institute for Congestion Reduction
University of South Florida
Center for Urban Transportation Research | University of South Florida

NICR
NATIONAL INSTITUTE F
CONGESTION REDUCTI

Disclaimer

The contents of this report reflect the views of the authors, who are responsible for the facts and the accuracy of the information presented herein. This document is disseminated in the interest of information exchange. The report is funded, partially or entirely, by a grant from the U.S. Department of Transportation's University Transportation Centers Program. However, the U.S. Government assumes no liability for the contents or use thereof.

Technical Report Documentation Page

1. Report No.	2. Government Accession No.	3. Recipient's Catalog No.	
4. Title and Subtitle Transit Priority		5. Report Date May 2023 6. Performing Organization Code	
7. Author(s) Saeid Soleimaniamiri, Xiaopeng Li, Keke Long		8. Performing Organization Report No.	
9. Performing Organization Name and Address Department of Civil and Environmental Engineering University of South Florida 4202 E Fowler Avenue, ENC 3300 Tampa, FL 33620		10. Work Unit No. (TRAIS) 11. Contract or Grant No. 69A3551947136, #79070-16 #79070-17	
12. Sponsoring Organization Name and Address U.S. Department of Transportation University Transportation Centers 1200 New Jersey Avenue, SE Washington, DC 20590 United States National Institute for Congestion Reduction 4202 E. Fowler Avenue Tampa, FL 33620-5375 United States		13. Type of Report and Period Covered Final Report, [August 10, 2020 – September 31, 2021] 14. Sponsoring Agency Code	
15. Supplementary Notes			
16. Abstract To establish an efficient way of improving the service quality of the public transportation system, this research seeks the optimal vehicle scheduling at a multi-conflict area considering heterogeneous vehicle headways and weighted by vehicle occupancies to minimize the total travel time delay cost while giving priority to transits with higher occupancy. A mixed-integer programming (MIP) model is proposed to solve the exact optimal solution to this problem and a customized branch-and-bound algorithm is designed to improve computational efficiency. A set of numerical experiments in various scenarios are tested to demonstrate the feasibility and effectiveness of the proposed model and algorithm. The comparison results show that coordination of vehicles with individual-vehicle-based control can significantly increase the capacity of the conflict area and reduce the delay of transits compared to existing well-known control strategies (e.g., stop signs and signals).			
17. Key Words Vehicle scheduling, connected automated vehicle (CAV), individual-vehicle based control, multi-conflict area, branch-and-bound algorithm		18. Distribution Statement	
19. Security Classification (of this report) Unclassified.	20. Security Classification (of this page) Unclassified.	21. No. of Pages 48	22. Price

Acknowledgments

This project was sponsored by the National Institute for Congestion Reduction (NICR) and financially supported by the U.S. National Science Foundation through Grants CMMI# 1558887 and #1932452.

Table of Contents

Figures

Tables

Executive Summary

Traffic conflict areas are a major cause of traffic incidents and congestion in urban road networks, which also results in delays of the urban public transit system. A conventional solution to this issue is to regulate traffic flows at a conflict area by traffic signs or signal timing. Although these control strategies can ensure that vehicles pass the conflict area safely and partially mitigate the traffic congestion, they still cannot eliminate the stop-and-go traffic. As a result, problems caused by stop-and-go traffic remain unaddressed, such as additional travel time delays, excessive fuel consumption, and throughput reduction. To solve this problem, this study utilizes the connected and automated vehicle (CAV) technique to design individual-vehicle-level scheduling. This study aims to address the research gaps in both fundamental methodologies and engineering applications on this general topic. The investigated problem seeks the optimal vehicle scheduling at a multi-conflict area considering heterogeneous vehicle headways and weighted by vehicle occupancies (thus giving priority to transits with higher occupancy) to minimize the total travel time delay cost. A mixed-integer programming (MIP) model is proposed to solve the exact optimal solution to this problem. Although small instances of the proposed model can be solved by existing commercial MIP solvers, their computational time increases almost exponentially as the number of vehicles and approaches increases. To ensure computational efficiency, we present a customized branch-and-bound algorithm that introduces a set of valid cuts to expedite the solution speed. Numerical experiments in various scenarios are tested to demonstrate the feasibility and effectiveness of the proposed model and algorithm. The comparison results show that coordination of vehicles with individual-vehicle-based control can significantly increase the capacity of the conflict area and reduce the vehicle travel time compared to existing well-known control strategies (e.g., stop signs and signals) while it is computationally tractable for real-world CAV applications. Further, we present two case studies of individual-vehicle-based control at a given conflict area for various arrival traffic demands. These results facilitate future urban traffic management with transit priority.

Chapter 1. Introduction

Transit Signal Priority (TSP) is a collection of techniques that help provide preference to transit buses at signalized intersections. TSP reduces the transit delay and results in better service quality of the public transportation system by adjusting the traffic signal plan according to transit status. As one of the most important approaches to promoting the public transportation system, TSP has been applied in most major cities around the world (Liao & Davis, 2007). At conflict areas, traffic control strategies, such as traffic signs or signal timing, are essential for regulating traffic flow and ensuring safe intersection operations. Transit priority, on the other hand, offers transit vehicles a higher level of treatment to minimize delays and enhance the stability of the transit system.

A reasonable TSP design needs to improve the overall performance of the traffic system. On the one hand, TSP needs to provide priority to delayed transit buses to avoid delays, thus improving the stability of the transit system. TSP also needs to reduce the impact of transit bus priority on other vehicles (Anderson et al., 2019; Hu et al., 2015, 2016). A detailed TSP design is needed for urban network bottlenecks such as intersections. However, the conventional solution to regulate traffic flows, including regular vehicles and transit buses at an intersection is by traffic signs or signal timing, especially at intersections with heavy traffic (Webster, 1958; Alcelik, 1981; Robertson et al., 1991; Mirchandani et al., 2001; Ceylan et al., 2004; Yin et al., 2008). Although these intersection control strategies regulating traffic flows can ensure that vehicles pass the conflict area safely and partially mitigate the traffic congestion, they still cannot eliminate the stop-and-go traffic. As a result, problems caused by stop-and-go traffic remain unaddressed, such as additional travel time delays, excessive fuel consumption, and throughput reduction.

Connected automated vehicle (CAV) technology offers a unique opportunity to solve the aforementioned problems by eliminating the stop-and-go traffic. Thanks to the availability of real-time vehicle arrival information and the capability to control vehicle trajectories under the connected and automated environment, vehicle scheduling at a conflict area can be precise to each individual vehicle. To be more specific, in a fully connected environment, a centralized controller can be deployed at the conflict area to receive all information about each individual CAV and accordingly determine their departure time to minimize the total travel time delay of all CAVs. With the defined departure time, CAVs can regulate their movements to pass the conflict area without stopping, which consequentially reduces fuel consumption. By optimizing the maximized intersection performance weighted by vehicle occupancies, the controller gives higher priority to transit. This way, non-stop intersection control can be proposed to benefit both the system and users by mitigating traffic congestion and eliminating (or alleviating) stop-and-go traffic. This research aims to address the existing research gaps in the CAV-based vehicle scheduling\signal optimization problem with a discrete modelling optimization framework. A mixed-integer programming (MIP) model is proposed to solve the exact optimal solution to the vehicle scheduling problem (VSO) problem (the optimization problem that selects an optimal departure sequence of vehicles at a conflict area) such that the total travel time delay cost of all vehicles passing the conflict area is minimized. The contributions of this study are summarized as follows. First, we propose an individual-vehicle-based control (IVC) model that can solve the optimal departure sequence of all CAVs at a multi-approach conflict area considering heterogeneous CAV headways and values of the time. Second, to efficiently solve this model, a customized branch-and-bound algorithm featured with the dynamic programming framework is proposed. Analysis of theoretical model properties yields a novel set of valid cuts that dramatically reduce the solution space of the proposed algorithm. Third, various numerical experiments are conducted to verify the effectiveness of the IVC

strategy and the proposed solution approach. Results show that the proposed customized algorithm obtains the exact optimal departure sequence of CAVs efficiently (compared with Gurobi, an existing commercial solver). This shows that the proposed solution approach is suitable for real-time CAV applications. Finally, the results confirm that the IVC strategy outperforms both the reservation-based control (RBC) and fixed-time signal control (FTSC) in terms of reducing total travel time delay costs. The proposed method establishes a methodological foundation for obtaining the exact optimal solution to a real-world vehicle scheduling optimization problem such as transit scheduling. This report also offers important insights about congestion reduction when planning future urban transportation system. They are also useful for transit agencies and traffic management centers to design transit priority strategies in the real world in the future.

Chapter 2. Literature Review

Connected automated vehicle (CAV) technology brings new control benefits to intersections. When all vehicles, including the transits, are CAVs, their status, including position, speed, and passenger account, can be sensed, and their trajectory can be controlled precisely. The trajectory of vehicles can be optimized in cooperation with signal planning. This problem can be abstract as an optimization problem to find the most efficient way to get vehicles through intersections without conflicts. Existing control strategies seek the optimal sequence of CAVs leaving a conflict area by applying either centralized or decentralized control. In decentralized control, each individual CAV approaching a conflict area determines its own operations based on the information received from the coordinator and/or other CAVs. Numerous decentralized control models have been proposed to coordinate CAVs at various conflict areas using heuristic- or optimization-based strategies (Rios-Torres and Malikopoulos, 2017). Heuristic-based strategies are proposed for increasing the throughput or reducing the average travel time delay of CAVs with virtual vehicle/platooning (Uno et al., 1999; Lu et al., 2000; Lu and Hedrick., 2003; Lu et al., 2004), fuzzy logic (Milanés et al., 2010; Milanés et al., 2011; Milanés et al., 2011; Onieva et al., 2012), and critical/invariant sets (Hafner et al., 2013; Qian et al., 2014; Colombo and Del Vecchio., 2015) for different roadway facilities (e.g., intersection, merging roadways, etc.). Although these control strategies validate the capability of CAV technologies in improving traffic operations in a conflict area, they are mostly ad-hoc methods without systematic optimization or theoretical insights. Further, various decentralized optimization frameworks have been proposed for intersections (Makarem et al., 2013; Campos et al., 2014; Kim et al., 2014; Qian et al., 2015; Le et al., 2015; Zhang et al., 2017; Malikopoulos et al., 2018) and merging roadways (Cao et al., 2015) considering different performance measures (e.g., minimizing travel time delay, acceleration, or the difference between the vehicle's actual speed and desired speed). In these optimization methods, each individual CAV solves its own optimization problem based on the information received from vehicles inside a specific area around its current position. While the short communication range required by decentralized control suits real-time applications, its solution might result in inferior traffic performance or even deadlocks. Moreover, the self-selectivity nature of this control approach prevents the system from achieving the maximum benefit of CAV technology.

A centralized controller, however, may maximize the system performance in terms of optimizing a systematic objective (e.g., minimizing total travel time delay, maximizing the throughput of the traffic flow at a conflict area, etc.) via determining the best departure sequence of all CAVs in the traffic stream. One classic centralized control mechanism is the reservation-based control (RBC) strategy proposed by Dresner and Stone (2004). In this strategy, each individual CAV sends a request to a centralized controller to reserve a time period at a conflict area. The centralized controller then coordinates CAVs based on their information and requests. Since then, numerous efforts using the RBC strategy have been made in the literature (Dresner and Stone, 2008; Au and Stone, 2010; de La Fortelle, 2010; Huang et al., 2012; Zhang et al., 2013). Assuming the first-in-first-out (FIFO) mechanism for CAVs to pass a conflict area, Lee and Park (2012) investigate an optimization problem to minimize the possible overlap of CAV trajectories at the conflict area. This work is extended to multiple intersections in a corridor system (Lee and Park, 2013). Further, Levin et al. (2017) optimize the CAV intersection trajectories by developing a new communication protocol for reservation policy. While these studies provide managerial insights about the system-level benefits of incorporating CAV technology to traffic operations, the intensive communication load, the possibility of having deadlocks in a solution, and the sub-optimality of the solution remain to be addressed.

One class of studies seeks for the optimal or near-optimal solution to vehicle coordination decisions at a conflict area considering various performance measures. Jin et al. (2012) propose a modified multi-agent system that aims to find te optimal departure sequence of CAVs. The simulation results showed that the proposed multi-agent system can improve the traffic system performance compared to the FIFO mechanism. Zhu et al. (2015) develop a linear programming model transformed from a bi-level optimization model to account for both CAV intersection control and dynamic traffic assignment. Li et al. (2018) propose a genetic-algorithm-based optimization method to decide the near-optimal passing sequence of CAVs at an intersection and calculate their optimal trajectories simultaneously. Yang et al. (2016) develop a branch-and-bound algorithm to sequentially optimize the signal timing plan and vehicle trajectories considering three different stages of technology development. A Dynamic programming (DP) algorithm is proposed by Wu et al. (2009) to determine the best access order of approaching CAVs to an intersection considering homogenous traffic flow yet heterogeneous vehicles' values of the time. The complexity of the proposed algorithm considering evacuation time as the objective function is shown no more than polynomial in the number of CAVs, but possibly exponential in the number of conflict approaches. As the complexity of the proposed DP algorithm increases with the increase in the number of conflicting approaches, they further propose an ant colony method to efficiently solve a large-scale vehicle scheduling optimization (VSO) problem to a near-optimum solution (Wu et al., 2012). Similarly, Yan et al. (2012) propose a branch-and-bound algorithm as well as a heuristic to evacuate all CAVs as soon as possible by determining their optimal passing order. To improve the computational complexity of the proposed branch-and-bound algorithm, they propose a fundamental mini-group algorithm by consolidating CAVs into clusters and decreasing the solution space. The problem formulation in this work is later extended to a corridor system containing multiple adjacent intersections (Yan et al., 2011; Yan et al., 2013). Further, Li and zhou (2017) develop a MIP model and a parallel branch-and-bound algorithm to optimally serve CAV requests at an intersection within a heterogeneous traffic environment comprised of both CAVs and human-driven vehicles. Recently, Yu et al. (2018) optimize the trajectories of the platoon of CAVs using the calculated optimal CAV arrival times. They use the state-of-the-art Gurobi solver to solve the proposed optimization model.

While these studies provide innovative solutions to this challenging problem, several critical issues in both fundamental methodologies and engineering applications are yet to be addressed. From the methodological perspective, solving the VSO problem to the exact optimal solution at a general conflict area remains a challenge due to not only the very complex nature of the scheduling problem but also the unique safety requirements of vehicle kinematics. To the best of our knowledge, no exact algorithm has been developed to solve the exact optimum of this complicated problem efficiently. From the application perspective, while most studies are intended for a simple conflict area with two approaches (e.g., a one-way intersection) with identical vehicles, which lacks the consideration of vehicles that should be given higher priority such as transit. Real-world traffic is comprised by multi-class vehicles with heterogeneous time headways and values of the time. Further, vehicles from more than two approaches may compete for the rights of way at a single conflict area (e.g., a multi-approach intersection, multilane highways merging into the same ramp). These problems in realistic traffic render many of the existing methods not directly applicable.

Chapter 3. Problem Statement and Model Formulation

This section formulates the VSO problem at a general conflict area considering heterogeneous vehicle time headways and values of time, which is applied to simulate the traffic with different kinds of vehicles and transit. The investigated problem and its parameters, variables, and assumptions are first formally introduced. Then, the VSO problem is formulated as a MIP model to minimize the total travel time delay cost.

Problem Statement

This study considers a problem involving multiple traffic approaches toward the same conflict area, as illustrated by Figure 1. Although a real-world conflict area might not always follow the same design, a number of traffic management problems at various conflict points can be represented or decomposed into the study VSO problem. For example, at the intersection illustrated in Figure 2, the four red dots denote conflict points, each with two conflicting one-lane approaches. Thus, the associated signal timing problem can be decomposed into four VSO problems, each associated with one conflict point. Building this foundation enables us to scale up the proposed solution technique to a real-world conflict area with a much more complicated design (e.g., multi-lane/multi-directions approaches).

A centralized controller schedules vehicles from all approaches to pass the conflict area, aiming to achieve the minimum total travel time delay. All the vehicles in this study are assumed to be individually controllable CAVs. The key notation is listed in Table 1.

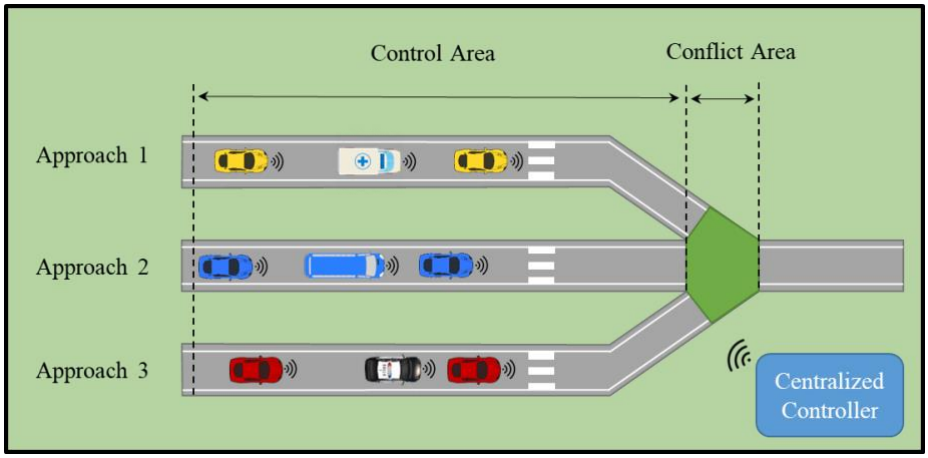

Figure 1. Conflict area with heterogeneous CAVs and a centralized controller.

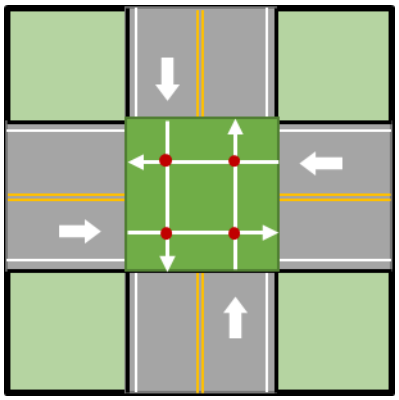

Figure 2. Real-world intersection (each red dot represents a conflict point in the investigated problem).

Table 1. Notation (VSO)

Parameters	Description
I	Number of the approaches
$\mathcal{I} \coloneqq 1, \dots, I$	Set of approaches
N_i	Number of CAVs in approach $i \in \mathcal{I}$
$\mathcal{N}_i \coloneqq 1, \dots, N_i$	Set of CAVs merging from approach $i \in \mathcal{I}$
$\bar{v}_i$	Free flow speed of approach $i \in \mathcal{I}$
x_{in}^0	Distance between CAV (i,n) and the conflict area at the scheduling time
t_{in}^-	Earliest departure time of CAV (i,n)
u_{in}	Value of travel time of CAV (i,n)
s_{in}	Jam spacing of CAV (i,n) and its preceding CAV
τ_{in}	Minimum time gap of CAV (i,n)
d_{in}	Minimum following time headway between CAV (i,n) and its preceding CAV
a_{in}	Arrival time headway between CAV (i,n) and its preceding CAV
cl_{ij}	Clearance time required for switching from approach $j \in \mathcal{I}$ to approach $i \in \mathcal{I}, i \neq j$
Decision variables	**Description**
t_{in}^+	Scheduled departure time of CAV (i,n)
$y_{in\ jm} \in 0,1$	$y_{in\ jm} = 1$ if CAV (i,n) pass the conflict area before CAV (j,m)

As shown in Figure 1, this study considers a conflict area formed by a set of one-lane approaches $\mathcal{I} \coloneqq \{1, \dots, I\}$ whose maximum speed (i.e. free flow speed) is $\bar{v}_i, \forall i \in \mathcal{I}$. In the control area of each approach $i \in \mathcal{I}$, a set of individually controllable CAVs ordered sequentially from downstream to upstream indexed with $\mathcal{N}_i \coloneqq 1, \dots, N_i$ are moving into and aim to pass the conflict area. The nth CAV ($n \in \mathcal{N}_i$) from approach i is denoted as a pair (i,n) that appears as subscripts in the following notation. Since the space of the conflict area is limited, CAVs arriving from different approaches at the same time cannot pass the conflict area simultaneously. Therefore, a centralized controller is deployed to schedule those CAVs from various approaches to safely pass the conflict area with the minimum system-level travel time delay cost by determining the scheduled departure time t_{in}^+ for each CAV (i,n). To consider

different types of vehicles, each CAV (i,n) is assumed to have its own value of time u_{in}. A CAV's value of time is related to its priority (e.g., an ambulance has a higher priority than a regular passenger car) and passenger load (e.g., the time value of a transit bus is the summation of those from all passengers on board). In practical applications, specific rules for determining the value of time can be designed based on the circumstances. Due to safety, each CAV (i,n) has a heterogeneous jam spacing s_{in} and a minimum time gap τ_{in} from its preceding CAV when passing the conflict area, depending on its physical (e.g., acceleration limits) and cyber (e.g., communication delays) limits. Below we summarize the basic settings for the CAV's running characteristics in this research:

- In the fully connected environment, the distance between each CAV (i,n) and the conflict area at the scheduling time is denoted by x_{in}^0, and its value of travel time u_{in} is known.
- Only one lane is considered on each approach i. We assume that overtaking is not allowed among CAVs from the same approach.
- Regardless of each CAV (i,n)'s travel speed within the control area, its earliest departure time, t_{in}^-, (i.e., the earliest time when CAV (i,n) can leave the conflict area) and its arrival time headway following its preceding CAV, a_{in}, can accurately be estimated by the central controller, considering the acceleration\deceleration and speed constraints.
- To maximize the traffic throughput at the conflict area, we assume that all CAVs pass the conflict area at free flow speed $\bar{v}_i$. Thus, the minimum time headway for CAV (i,n) to follow another CAV at the conflict area is defined as $d_{in} = \tau_{in} + s_{in}/\bar{v}_i$. Basically, the centralized controller imposes a minimum following time headway d_{in} for two consecutive CAVs $(n-1, n \in \mathcal{N}_i \backslash \{1\})$ from the same approach $i \in \mathcal{I}$ to avoid collision at the conflict area.
- The minimum following time headway for CAV (i,n) following CAV $(j \neq i, m)$ from another approach takes an extra clearance time cl_{ij} due to switching approaches. Note that this notation allows heterogeneous time headways between different CAV pairs, depending on the CAV features (e.g., vehicle length) and driving rules (e.g., following gap settings).

Model Formulation

The VSO problem is formulated as a mixed-integer programming model that schedules all CAVs to safely pass a general conflict area from different approaches while minimizing the total travel time delay cost. The decision variables in this model are the scheduled departure time of each CAV (i,n), t_{in}^+, and a set of binary variables $y_{in\ jm}$ that specify the passing order between each two CAVs (i,n) and (j,m) from different approaches $i \neq j$. Binary variable $y_{in\ jm}$ equals to 1 if CAV (i,n) passes the conflict area before CAV (j,m) or 0 otherwise. These are necessary to account for heterogeneous headways that depend on CAV passing orders. To mathematically formulate this model, each CAV (i,n) shall satisfy the following sets of constraints.

- **Departure time constraints:** Due to the speed limit, no CAVs can drive along with the approach with a speed higher than the free flow speed. Thus, a CAV (i,n) cannot pass the conflict area earlier than its earliest departure time t_{in}^-, that is,

$$t_{in}^+ \geq t_{in}^-, \forall i \in \mathcal{I}, n \in \mathcal{N}_i \tag{1}$$

- **Following time headway constraints:** The time headway between two consecutive CAVs from the same approach when passing the conflict area should not be less than the minimum following time headway to avoid rear-end collisions, that is,

$$t_{in}^{+} - t_{i(n-1)}^{+} \geq d_{in}, \forall i \in \mathcal{I}, n \in \mathcal{N}_i \backslash \{1\} \tag{2}$$

- **Switching time headway constraints:** Likewise, the time headway between two CAVs from different approaches when passing the conflict area should not be less than the minimum following time headway of the following CAV plus an extra clearance time to avoid side collisions, that is,

$$t_{in}^{+} - t_{jm}^{+} + M y_{in\,jm} \geq d_{in} + cl_{ij}, \forall i < j \in \mathcal{I}, \forall n \in \mathcal{N}_i, m \in \mathcal{N}_j \tag{3}$$

$$t_{jm}^{+} - t_{in}^{+} + M\left(1 - y_{in\,jm}\right) \geq d_{jm} + cl_{ji}, \forall i < j \in \mathcal{I}, n \in \mathcal{N}_i, m \in \mathcal{N}_j \tag{4}$$

where M is a sufficiently large positive number. Note that the value of M must be greater than the maximum possible difference between the scheduled departure times of any two CAVs. To satisfy this condition, we simply set $M = \sum_{i \in \mathcal{I}}\left(t_{iN_i}^{-} - t_{i1}^{-} + a_{i1}\right) + \left(\sum_{i \in \mathcal{I}} N_i - 1\right).\max_{i,j \in \mathcal{I}}\{cl_{ij}\}$.

- **Overtaking prohibition constraints:** These constraints are imposed since CAVs from the same approach are not allowed to overtake each other. They basically prevent a CAV (i, n) from passing the conflict area earlier than its proceeding CAVs in the same approach, that is,

$$y_{in\,jm} \geq y_{in\,j(m-1)}, \forall i < j \in \mathcal{I}, n \in \mathcal{N}_i, m \in \mathcal{N}_j\{1\} \tag{5}$$

$$y_{in\,jm} \leq y_{i(n-1)\,jm}, \forall i < j \in \mathcal{I}, n \in \mathcal{N}_i\{1\}, m \in \mathcal{N}_j \tag{6}$$

It is noteworthy that these valid inequalities are redundant to the departure time constraints and the fact that a CAV's earliest departure time cannot be smaller than its preceding CAV's earliest departure time. Despite the redundancy, we keep them in the model since they may help expedite the solution speed.

Further, each CAV is associated with one operational cost as follows.

- **Travel time delay cost:** The travel time delay cost of each CAV (i, n) is affected by the CAV's scheduled departure time t_{in}^{+}, and value of time u_{in}. The CAV's scheduled departure time itself depends on the departure sequence of all preceding CAVs decided by the central controller. Let $D_{in}(t_{in}^{+})$ denote the travel time delay cost of CAV (i, n), which is defined as the product of its value of time u_{in} and travel time delay. Using a centralized controller, the earliest departure time of each CAV (i, n) can be accurately predicted and will be used as the reference point for calculating the travel time delay cost of CAV. With this, the travel time delay cost of CAV (i, n) is formulated as follows.

$$D_{in}(t_{in}^{+}) = u_{in} * (t_{in}^{+} - t_{in}^{-}), \forall i \in \mathcal{I}, n \in \mathcal{N}_i \tag{7}$$

Now we formulate the VSO problem as

$$VSO: \min_{t_{in}^{+} \in (t_{in}^{-}, \infty)} O^{VSO}(t_{in}^{+}) \coloneqq \sum_{i \in \mathcal{I}} \sum_{n \in \mathcal{N}_i} D_{in}(t_{in}^{+}) \tag{8}$$

Subject to Constraints (1)–(6). Note that this mixed-integer programming model formulation can be used in other modes of scheduling optimization problems where only the arrival/departure times of a set of fleets need to be determined (e.g., aircraft landing scheduling at a single runway, train platforming, etc).

As it is mentioned earlier, one major obstacle to IVC strategy is the problem complexity as vehicles are considered individually. The following proposition discusses the complexity of the VSO problem.

Proposition 1. VSO is an NP-hard problem.

Proof. The NP-hardness of VSO can be proven by showing that the single machine scheduling problem subject to chain-like precedence and release date constraints denoted by $1|chain, r_j|\sum w_j C_j$, which is shown by (Lenstra et al., 1977) to be NP-hard, can be reduced to VSO problem in a polynomial time. A generic $1|chain, r_j|\sum w_j C_j$ problem instance is stated as follows. Given N jobs $\mathcal{J} \coloneqq \{J_1, \dots, J_N\}$ that are partitioned into G groups, $\mathcal{G} \coloneqq \{1, \dots, G\}$, and have to be processed on a *single machine*, which can execute at most one job at a time, the problem is to find the feasible schedule of jobs that corresponds to the lowest weighted completion time. Each group of jobs $g \in \mathcal{G}$ includes M_g jobs, $\mathcal{M}_g \coloneqq \{1, \dots, M_g\}$, where $N = \sum_{g\in\mathcal{G}} M_g$ is the total number of jobs. Jobs of the same group have to be processed contiguously. Each job $(g \in \mathcal{G}, m \in \mathcal{M}_g)$, is associated with a priority w_{gm}, a processing time p_{gm}, a release date r_{gm} (i.e., the earliest time a job can start to be processed), and a completion time C_{gm}, which can be calculated based on the completion time of preceding job in a given schedule and the job's release date. We can easily transform this problem instance into an equivalent VSO problem instance. Note that the VSO problem is a general case of $1|chain, r_j|\sum w_j C_j$ problem since it also considers a clearance time when switching from one approach to another. Considering the conflict point as a single machine and CAVs as jobs, we can do such a transformation by setting $\mathcal{I} = \mathcal{G}$, $\mathcal{N}_i = \mathcal{M}_g$, $u_{in} = w_{gm}$, $d_{in} = p_{gm}$, $(t_{in}^- - h_{in}) = r_{gm}$, $t_{in}^+ = C_{gm}$, and $cl_{ij} = 0, \forall i \neq j \in \mathcal{I}, n \in \mathcal{N}_i, g \in \mathcal{G}, m \in \mathcal{M}_g$. With this transformation, we can say the optimal solution to the VSO problem instance also solves the $1|chain, r_j|\sum w_j C_j$ instance to the optimum. Obviously, this transformation between the $1|chain, r_j|\sum w_j C_j$ and VSO problem only takes a polynomial number of operations. This proves the NP-hardness of VSO problem. □

Proposition 1 proves that there is no efficient (or polynomial-time) algorithm that can always solve a general instance of the VSO problem. To draw a deeper insight into the complexity of the VSO problem, the following proposition investigates the size of the feasible region of the proposed model.

Proposition 2. Model (1)–(8) has a total number of $\frac{(\sum_{i\in\mathcal{I}} N_i)!}{\prod_{i\in\mathcal{I}}(N_i!)}$ feasible solutions.

Proof. The number of CAV passing sequences at a conflict area with I approaches is $(\sum_{i\in\mathcal{I}} N_i)!$ if overtaking is allowed (and thus CAV orders can be arbitrarily permuted even in the same approach). Note that in these sequences, among $(N_i!)$ Permutations for each approach i, only one permutation is consistent with the input CAV sequence without overtaking for this approach. And thus, among $\prod_{i\in\mathcal{I}}(N_i!)$ sequences with different permutations yet the same combination of CAV passing orders in the same approach, only one sequence is consistent with the input CAV sequence without overtaking for all approaches and all other sequences have overtaking and thus are infeasible. Thus, the number of all feasible sequences is equal to $\frac{(\sum_{i\in\mathcal{I}} N_i)!}{\prod_{i\in\mathcal{I}}(N_i!)}$. This completes the proof.

Proposition 2 suggests that the complexity of using simple enumeration to solve the VSO problem increases exponentially, as the number of CAVs and approaches increase. To solve such a complex problem efficiently, we propose a customized branch-and-bound algorithm in the following section.

Chapter 4. Branch-and-Bound Algorithm

The MIP model presented in the previous section can be solved with existing state-of-the-art commercial solvers (e.g., Gurobi) to the exact optimal solution(s). However, this may require excessive computational resources for large-scale problem instances, as the solution space increases exponentially with the instance size (see Proposition 2). Thus, it is imperative to develop a customized algorithms with appealing computational performance. To this end, this section presents a customized branch-and-bound (B&B) algorithm to solve the investigated problem. This section first introduces the parameter settings and the procedure of the B&B algorithm. Then, the computation method of the lower bound and upper bound costs of a node in the B&B tree is presented. Finally, a set of valid cuts is proposed to expedite the algorithm by reducing the solution space.

The B&B algorithm is an enumerative optimization method that solves a discrete optimization problem by breaking down the feasible solution space into smaller subregions, and calculating the bounds for each subregion successively until the optimal solution is found (Little et al., 1963). For each subregion, the lower and upper bounds are obtained by solving an easier (or relaxed) problem and finding a feasible solution to the original problem, respectively. The best lower and upper bounds found at each iteration are used to update the global lower and upper bounds, respectively. The procedure ends when the lower bound of a subregion produces a feasible solution or no better solution than those already found exists. The key notation of the B&B algorithm is listed in Table 2.

Table 2. Notation (B&B)

Parameters	Description
L	Number of the approaches
$\mathcal{L} \coloneqq 0,1,\dots,L$	Set of all levels
M_l	Number of nodes at level $l \in \mathcal{L}$
$\mathcal{M}_l \coloneqq 1,\dots,M_l$	Set of all nodes at level $l \in \mathcal{L}$
K_l	Total number of options for choosing l passed CAVs (PVs) from all approaches at level $l \in \mathcal{L}$
$\mathcal{K}_l \coloneqq \{1,\dots,K_l\}$	Set of all different combinations of PVs from all approaches at level $l \in \mathcal{L}$
$\mathcal{G}_{lk}$	Set of nodes at level $l \in \mathcal{L}$ with combination set $k \in \mathcal{K}_l$
R_{lmi}	Number of PVs from approach $i \in \mathcal{I}$ at node (l,m)
$\mathcal{R}_{lmi} \coloneqq \{0,1,\dots,R_{lmi}\}$	Set of all PVs from approach $i \in \mathcal{I}$ at node (l,m)
$\mathcal{Q}_{lmi} \coloneqq \mathcal{N}_i \backslash \mathcal{R}_{lmi}$	Set of all approaching CAVs (AVs) from approach $i \in \mathcal{I}$ at node (l,m)
J_{lm}	Last PV's approach index at node (l,m)
P_{lm}	Index of the parent node of node (l,m)
C_{lm}^{PV}	Travel time delay cost of PVs at node (l,m)
C_{lmi}^{AV}	Minimum travel time delay cost of AVs from approach $i \in \mathcal{I}$ at node (l,m)
C_{lm}^{LB}	Travel time delay cost of AVs at node (l,m) solving relaxed problem
C_{lm}^{UB}	Travel time delay cost of AVs at node (l,m) given a feasible solution
LB_{lm}	Lower bound of node (l,m)
UB_{lm}	Upper bound of node (l,m)
GLB	Global lower bound
GUB	Global upper bound

Figure 3 illustrates the key notation. The B&B algorithm solves the VSO problem by breaking down the feasible region into $L = \sum_{i \in \mathcal{I}} N_i$ levels, indexed as $\mathcal{L} \coloneqq 1,\dots,L$. Each level $l \in \mathcal{L}$ contains all feasible sub-solutions to the sequence of the first l CAVs passing the conflict area, which are denoted as $\mathcal{M}_l \coloneqq 1,\dots,M_l$. For convenience, we refer the set of CAVs already passing the conflict area the passed vehicles (PV). Each sub-solution $m \in \mathcal{M}_l$ is a *node* of the B&B tree at level l. The mth node ($m \in \mathcal{M}_l$) from level l is denoted as a pair (l,m) that appears as subscripts in the following notation. Note that the PVs at each level l can be chosen differently from all approaches. At a node (l,m), the combination of PVs from different approaches may differ from the ones at node (l,p), $\forall p \neq m \in \mathcal{M}_l$. With this, the nodes at each level l can be grouped into smaller subsets $\mathcal{G}_{lk}, \forall k \in \mathcal{K}_l$ that each has the same combination of the first l PVs from different approaches, where $\mathcal{K}_l \coloneqq \{1,\dots,K_l\}$ denotes the set of all feasible combinations of choosing the first l PVs from different approaches. Note that while all nodes in the same subset $\mathcal{G}_{lk}$ contain the same set of PVs, they have different passing sequences. With these, we denote $\mathcal{R}_{lmi} \coloneqq \{0,1,\dots,R_{lmi}\}$ as the set of PVs from approach i. Then let $\mathcal{Q}_{lmi} \coloneqq \mathcal{N}_i \backslash \mathcal{R}_{lmi}$ denote the set of CAVs approaching to the conflict area on approach i that are not scheduled yet, which we refer as approaching CAVs (AV). Let J_{lm} denote the last PV's approach index at each node (l,m).

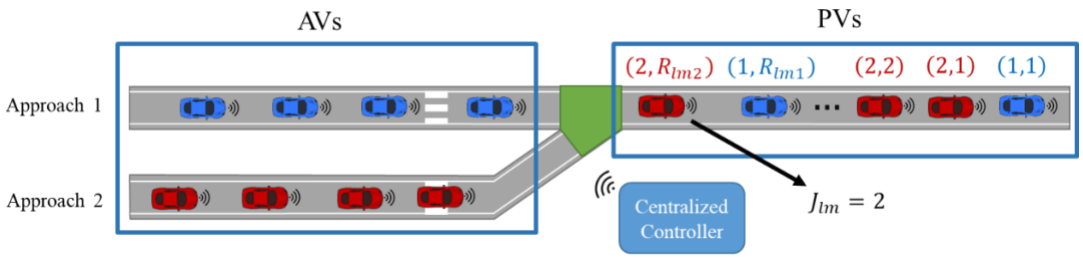

(a) Illustration of the PVs' and AVs' sets, $R_{lmi}, \forall i \in \mathcal{I}$, and J_{lm} at a given node

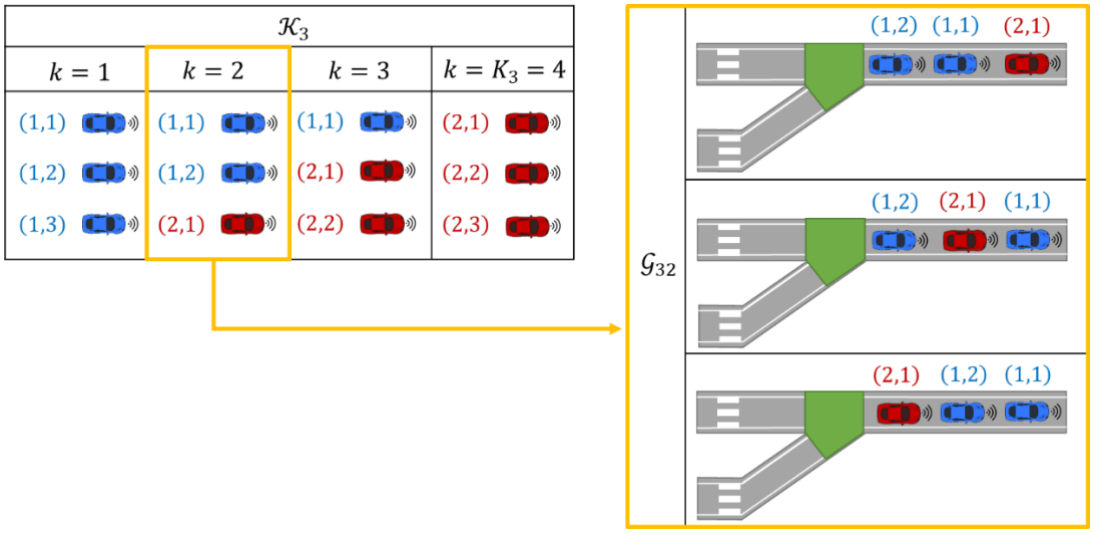

(b) An illustrative example of the sets $\mathcal{K}_l$ and $\mathcal{G}_{lk}$ at level 3 of the B&B tree

Figure 3. An illustration to the B&B notation.

Each node (l, m) is constructed from its parent node $P_{(l-1)m} \in \mathcal{M}_{(l-1)}$ at previous level $l-1$ in the branching procedure. Further, each node (l, m) is associated with a travel time delay cost, C_{lm}^{PV}, of its PV set. The PVs' passing order at each node (l, m) may change the boundary of an AV $(i \in \mathcal{I}, n \in \mathcal{Q}_{lmi})$'s possible departure time in Constraint (1) from its earliest departure time t_{in}^{-} to a higher value $t_{in\,lm}^{*}$. As a result, the set of AVs from each approach i at a node (l, m) may also be associated with a minimum amount of travel time delay cost, C_{lmi}^{AV}. The lower bound LB_{lm} and upper bound UB_{lm} of a node (l, m) then is formulated as:

$$LB_{lm} = C_{lm}^{PV} + C_{lm}^{LB}, \forall l \in \mathcal{L}, m \in \mathcal{M}_l \tag{9}$$

$$UB_{lm} = C_{lm}^{PV} + C_{lm}^{UB}, \forall l \in \mathcal{L}, m \in \mathcal{M}_l \tag{10}$$

where C_{lm}^{LB} and C_{lm}^{UB} are the travel time delay costs in a simpler relaxed VSO problem and in a feasible solution to the original VSO problem considering the set of AVs at node (l, m), respectively. To store the best solution found so far, we define GLB and GUB as the global lower and upper bounds to the original VSO problem, respectively.

With these definitions, the algorithm starts from an initial node $(0, 0)$ where $R_{00i} = 0, \forall i \in \mathcal{I}$. Then, I number of child nodes are constructed by adding the first AV from $\mathcal{Q}_{00i}$ from each approach $i \in \mathcal{I}$ to set $\mathcal{R}_{00i}$, respectively. After adding the lower and upper bounds of each constructed child node to the

lower bound list $List^{LB}$ and upper bound list $List^{UB}$, respectively, and deleting the bounds of their parent node from these lists, the GLB and GUB will be updated. Then, the algorithm repeats this procedure by branching over the node with the lowest lower bound in $List^{LB}$. As the procedure continues, the GLB converges to the GUB. To accelerate this convergence rate, each created child node is checked for pruning through a set of valid cuts. The algorithm terminates when either GLB and GUB are converged or the given time limit is reached.

In the following subsections, we first illustrate the procedure of updating C_{lm}^{PV} at each constructed child node. Then, the procedure of calculating C_{lm}^{LB} and C_{lm}^{UB} at each node (l, m) is provided. Finally, a set of valid cuts is presented to reduce the feasible solution space.

Cost of a Node

The C_{lm}^{PV} at each node (l, m) is the sum of the travel time delay cost of all CAVs that have already been scheduled (i.e., the set of PVs) at that node. Therefore, it can be calculated by adding the travel time delay cost of the newly added CAV, $R_{lm(J_{lm})}$, to the travel time delay cost of all CAVs that are already passed (i.e., the travel time delay costs of PVs of its parent node $C_{(l-1)P_{lm}}^{PV}$). To minimize the travel time delay cost of CAV $R_{lm(J_{lm})}$, we schedule the CAV to pass the conflict area at the earliest possible departure time. With this, the scheduled departure time of the CAV $R_{lm(J_{lm})}$ at node (l, m) is formulated as follows.

$$t^{+}_{(J_{lm})\left(R_{lm(J_{lm})}\right)} = \max t^{-}_{(J_{lm})\left(R_{lm(J_{lm})}\right)}, t^{+}_{\left(J_{(l-1)(P_{lm})}\right)\left(R_{(l-1)(P_{lm})\left(J_{(l-1)(P_{lm})}\right)}\right)} + d_{(J_{lm})(R_{lmi})} + cl_{(J_{lm})\left(J_{(l-1)(P_{lm})}\right)}, \forall l \in \mathcal{L}, m \in \mathcal{M}_l \tag{11}$$

where $t^{+}_{\left(J_{(l-1)(P_{lm})}\right)\left(R_{(l-1)(P_{lm})\left(J_{(l-1)(P_{lm})}\right)}\right)}$ is the scheduled departure time of the last PV at the parent node P_{lm}. Then, adding the travel time delay cost of the CAV $R_{lm(J_{lm})}$ to the cost of its parent node P_{lm} yields the travel time delay cost of node (l, m) as follows.

$$C_{lm}^{PV} = C_{(l-1)(P_{lm})}^{PV} + D_{(J_{lm})(R_{lmi})}\left(t^{+}_{(J_{lm})(R_{lmi})}\right), \forall l \in \mathcal{L}, m \in \mathcal{M}_l \tag{12}$$

Lower Bound

The lower bound of each node (l, m) in the B&B tree is calculated by adding the travel time delay cost of the PVs at that node, C_{lm}^{PV}, to the lower bound cost of all AVs (i.e. set Q_{lmi}), denoted by C_{lm}^{LB}. The formulation to calculate C_{lm}^{PV} has been presented previously, so here we focus on formulating the lower bound cost C_{lm}^{LB}. To reach this end, we consider a relaxed problem where all AVs are assumed to be homogeneous. Specifically, all AVs share the lowest value of time and minimum time headway among themselves, and no clearance time is considered when switching from one approach to another. This setting indicates that the optimal solution to the homogeneous VSO problem always results in lower travel time delay cost than any feasible solution to the original VSO problem and thus provides a lower bound cost of AVs at a given node. The following proposition presents the analytical solution to the homogeneous VSO problem.

Proposition 3. The first-in-first-out (FIFO) solution is the exact optimal solution to the homogeneous VSO problem.

Proof. Let assume a set of F CAVs from all approaches ordered sequentially form the downstream to the upstream $\mathcal{F} \coloneqq 1, \dots, F$, are moving to and aim to pass the conflict area. Let $f \in \mathcal{F}$ denote the fth CAV in the set, and denote the minimum time headway between each two consecutive CAVs and minimum time value by $\hat{d}$ and $\hat{u}$, respectively. Note that, there is no switching time headway in the homogeneous case and all CAVs share the same minimum time headway and value of time. Now let consider two consecutive CAVs f and $(f-1)$, where $f \in \mathcal{F}\backslash\{1\}$, and $t_f^- < t_{f-1}^-$. For a given passing order of all other CAVs, we investigate the effect of switching the position of these two CAVs on the total travel time delay cost. To do so, we first formulate the travel time delay costs of both cases for these two CAVs as follows.

$$D^O = \hat{u}.\left(t_{f-1}^{+,O} - t_{f-1}^-\right) + \hat{u}.\left(\max\left\{t_f^-, t_{f-1}^{+,O} + \hat{d}\right\} - t_f^-\right)$$

$$D^S = \hat{u}.\left(t_f^{+,S} - t_f^-\right) + \hat{u}.\left(\max\left\{t_{f-1}^-, t_f^{+,S} + \hat{d}\right\} - t_{f-1}^-\right)$$

where superscripts O and S represent the original and switched ordered of passing, respectively, and D represents the travel time delay cost of CAVs f and $f-1$. Now since $t_f^- < t_{f-1}^-$, we know that $t_f^{+,S} \leq t_{f-1}^{+,O}$. Further, from $t_f^- < t_{f-1}^- \leq t_{f-1}^{+,O}$, it is easy to obtain $t_f^- \leq t_{f-1}^{+,O} + \hat{d}$ and thus, $\max\left\{t_f^-, t_{f-1}^{+,O} + \hat{d}\right\} = t_{f-1}^{+,O} + \hat{d}$. Finally from $t_f^{+,S} \leq t_{f-1}^{+,O}$ and $t_{f-1}^- \leq t_{f-1}^{+,O}$ we can show that $\max\left\{t_{f-1}^-, t_f^{+,S} + \hat{d}\right\} \leq t_{f-1}^{+,O} + \hat{d}$ and thus, $D^S \leq D^O$. This implies that switching each two consecutive CAVs f and $(f-1)$ sequentially when $t_f^- < t_{f-1}^-$, not only decreases the sum of travel time delay costs of these two CAVs, but also decreases the second CAV's departure time which provides more space for the following CAVs to enjoy a lower travel time delay cost. This switching technique results to the FIFO solution that is shown to be optimal to the homogeneous VSO problem. This completes the proof. □

Proposition 3 indicates that the FIFO solution is the true optimum to the homogeneous VSO problem. With this analytical result, we can obtain the lower bound to a node in almost no time. Now let $\mathcal{F}_{lm} \coloneqq 1, \dots, L - \sum_{i \in \mathcal{I}} R_{lmi} + 1$ be the set of last PV , $R_{lm(J_{lm})}$, and all AVs' indexes in the FIFO order at a node (l, m), where $f \in \mathcal{F}_{lm}$ corresponds to the fth CAV in the set and i_f and n_f are the fth CAV's approach index and position in the original set $\mathcal{N}_i$, respectively. We also define $\hat{d}_{lm}$ and $\hat{u}_{lm}$ as the lowest minimum time headway and time value among all AVs, respectively. With these, C_{lm}^{LB} of each node (l, m) is formulated as follows.

$$C_{lm}^{LB} = \hat{u}_{lm} * \sum_{f \in \mathcal{F}_{lm}\backslash\{1\}} \left(\max\left\{t_{i_f n_f}^-, t_{i_{(f-1)} n_{(f-1)}}^+ + \hat{d}_{lm}\right\} - t_{i_f n_f}^-\right), \forall l \in \mathcal{L}, m \in \mathcal{M}_l \tag{13}$$

Note that $t_{i_1 n_1}^+$ in the above equation represents the scheduled departure time of last PV, $R_{lm(J_{lm})}$. Further, the lower bound of each node (l, m) is calculated using Equations (9), (12), and (13).

Upper Bound

The upper bound of each node (l, m) in the B&B tree is derived by adding the travel time delay cost of the PVs at that node, C_{lm}^{PV}, to the upper bound cost of all AVs at that node (i.e. set $\mathcal{Q}_{lmi}$), denoted by C_{lm}^{UB}. Although any feasible solution of AVs can be used to calculate the upper bound cost, it is important to create a feasible solution whose objective value is close to the true optimum for the sake of computational performance. To reach this end, this subsection presents a fast heuristic to obtain a good upper bound cost efficiently.

At a given a passing sequence of PVs decided by the centralized controller, the conflict area is occupied for a certain amount of time (i.e., $t^{+}_{(J_{lm})\left(R_{lm(J_{lm})}\right)}$), which is the last PV's departure time at node (l, m)). This occupation affects the possible departure time boundary of AVs and consequently, their travel time delay costs. Basically, an AV's possible departure time boundary may change from its earliest departure time to a higher value given the passing sequence of PVs ahead. This new boundary of an AV $(i \in \mathcal{I}, n \in \mathcal{Q}_{lmi})$ denoted by $t^{*}_{in\ lm}$, at each node $(l \in \mathcal{L}\backslash\{L\}, m \in \mathcal{M}_l)$ is formulated as follows.

$$t^{*}_{in\ lm} = \begin{cases} \max\left\{t^{-}_{in}, t^{+}_{(J_{lm})\left(R_{lm(J_{lm})}\right)} + d_{in} + cl_{i(J_{lm})}\right\} & n = R_{lmi} + 1 \\ \max\left\{t^{-}_{in}, t^{*}_{i(n-1)\ lm} + d_{in}\right\} & n > R_{lmi} + 1 \end{cases} \quad \forall l \in \mathcal{L}\backslash\{L\}, m \in \mathcal{M}_l, i \in \mathcal{I}, n \in \mathcal{Q}_{lmi} \tag{14}$$

As an AV (i, n)'s possible departure time boundary changes from t^{-}_{in} to $t^{*}_{in\ lm}$, its minimum travel time delay cost changes from zero to $u_{in}(t^{*}_{in\ lm} - t^{-}_{in})$. With this, the minimum travel time delay cost of the AVs from each approach $i \in \mathcal{I}$ at node $(l \in \mathcal{L}\backslash\{L\}, m \in \mathcal{M}_l)$ is formulated as follows.

$$C_{lmi}^{AV} = \sum_{n \in \mathcal{Q}_{lmi}} D_{in}(t^{*}_{in\ lm}), \forall l \in \mathcal{L}\backslash\{L\}, m \in \mathcal{M}_l, i \in \mathcal{I} \tag{15}$$

With this, we construct a feasible solution of the AVs with an iterative procedure. At each iteration, we let a single AV pass the conflict area such that the increase in the summation of minimum travel time delay cost of the rest of AVs from all approaches is minimized. This iterative procedure can be formally stated as the pseudocode in Algorithm 1.

Algorithm 1. Upper Bound Fast Heuristic Algorithm

Input: $I; \mathcal{J}; N_i, \mathcal{N}_i, \forall i \in \mathcal{J}; \mathcal{L}; \mathcal{M}_l, \forall l \in \mathcal{L}; J_{lm}, \forall l \in \mathcal{L}, m \in \mathcal{M}_l; R_{lmi}, \mathcal{Q}_{lmi}, \forall l \in \mathcal{L}, m \in \mathcal{M}_l, i \in \mathcal{J}$

$num \leftarrow \sum_{i \in \mathcal{J}} (N_i - d)$
$C \leftarrow 0$
While $(num > 0)$ **do**
  For $i \in \mathcal{J}$ **do**
    If $(R_{lmi} < N_i)$ **do**
      $t^{+}_{i(R_{lmi}+1)} \leftarrow t^{*}_{i(R_{lmi}+1)\, lm}$
      $R^{*}_{lmi} \leftarrow R_{lmi} + 1$
      $\mathcal{Q}^{*}_{lmi} \leftarrow \mathcal{Q}_{lmi} \backslash \{R^{*}_{lmi}\}$
      Determine $t^{*}_{in\, lm}, \forall n \in \mathcal{Q}^{*}_{lmi}$ from equation (14) using R^{*}_{lmi} and $J_{lm} = i$
      $\text{cost}^{\min}(i) \leftarrow \sum_{i \in \mathcal{J}} \left(C^{AV}_{lmi}\right)$ from equation (15) using $\mathcal{Q}^{*}_{lmi}$
    Else do
      $\text{cost}^{\min}(i) \leftarrow +\infty$
    End
  End for
  Find the minimum cost in list $\text{cost}^{\min}$ and set i^{*} as the index of minimum cost
  $C \leftarrow C + D_{i^{*}(R_{lmi^{*}}+1)}\left(t^{+}_{i^{*}(R_{lmi^{*}}+1)}\right)$
  $J_{lm} \leftarrow i^{*}$
  $R_{lmi^{*}} \leftarrow R_{lmi^{*}} + 1$
  $\mathcal{Q}_{lmi^{*}} \leftarrow \mathcal{Q}_{lmi^{*}} \backslash \{R_{lmi^{*}}\}$
  $num \leftarrow num - 1$
End while

Output: C

Valid Cuts

To improve the efficiency of the presented B&B algorithm, we add a set of valid cuts derived from the theoretical properties of the investigated problem to prune possible branches in the B&B tree. As mentioned in previous section, the boundaries of the AVs' possible departure times at a given node may change due to the passing sequence of PVs ahead. The new departure time boundary of an AV (i, n), $t^{*}_{in\, lm}$, and the minimum travel time delay cost of AVs from each approach i at a given node (l, m) is formulated in Equations (14) and (15), respectively. With these, the following proposition specifies a set of valid cuts to improve the efficiency of the B&B algorithm.

Proposition 4. For two nodes $(l \in \mathcal{L}\backslash\{L\}, k \in \mathcal{K}_l, m \in \mathcal{G}_{lk})$ and $(l \in \mathcal{L}\backslash\{L\}, k \in \mathcal{K}_l, p \in \mathcal{G}_{lk})$ in the same subset $\mathcal{G}_{\text{lk}}$, if $t^{*}_{i(R_{lmi}+1)lm} \leq t^{*}_{i(R_{lpi}+1)lp}$ and $C^{PV}_{lm} + C^{AV}_{lmi} \leq C^{PV}_{lp} + C^{AV}_{lpi}$, $\forall i \in \mathcal{I}$, then node $(l \in \mathcal{L}\backslash\{L\}, k \in \mathcal{K}_l, p \in \mathcal{G}_{lk})$ is dominated by node $(l \in \mathcal{L}\backslash\{L\}, k \in \mathcal{K}_l, m \in \mathcal{G}_{lk})$ and can be pruned from the B&B tree.

Proof. Please note that all nodes in the same level $l \in \mathcal{L}$ and subset $\mathcal{G}_{lk}$, $k \in \mathcal{K}_l$, contain the same set of PVs while their passing order is different. Note that if $t^{*}_{i(R_{lmi}+1)lm} \leq t^{*}_{i(R_{lpi}+1)lp}$, $\forall i \in \mathcal{I}$, from Equation (14) we know that $t^{*}_{in\, lm} \leq t^{*}_{in\, lp}$, $\forall n \in \mathcal{Q}_{lmi}$. Note that $t^{*}_{in\, lm}$ would be the same as $t^{*}_{in\, lp}$ for an AV

$(i \in \mathcal{I}, n \in \mathcal{Q}_{lmi})$ only if $t^*_{in\ lm} = t^*_{in\ lp} = t^-_{in}$ or $t^*_{i(R_{lmi}+1)lm} = t^*_{i(R_{lpi}+1)lp}$. Let denote the first AV from each approach $i \in \mathcal{I}$ where $t^*_{in\ lm} = t^*_{in\ lp}$ (if it happens) by N^*_i. According to Equations (14)-(15), we formulate the difference between C^{AV}_{lmi} and C^{AV}_{lpi} for each approach $i \in \mathcal{I}$ as follows.

$$\Delta C_{lpmi} = C^{AV}_{lpi} - C^{AV}_{lmi} = \left(t^*_{i(R_{lpi})lp} - t^*_{i(R_{lmi})lm}\right). \sum_{n \in \{R_{lmi}, \dots, N^*_i - 1\}} (u_{in}), \forall i \in \mathcal{I}$$

Now let consider the set of AVs in a given feasible passing sequence from the downstream to the upstream $\mathcal{F} := 1, \dots, L - \sum_{i \in \mathcal{I}} R_{lmi}$, where $f \in \mathcal{F}$ corresponds to the fth CAV in the set and i_f and n_f are the approach's index and position of the fth AV in the original set $\mathcal{N}_i$, respectively. With this, we formulate the actual departure time of AVs given the passing order in the set $\mathcal{F}$ for a given node (l, m) as follows.

$$\mathrm{t}^+_{i_f n_f\ lm} = \begin{cases} t^*_{i_f n_f\ lm} & f = 1 \\ \max\left\{t^*_{i_f n_f\ lm}, \mathrm{t}^+_{i_{(f-1)} n_{(f-1)}\ lm} + d_{i_f n_f} + cl_{i_f i_{(f-1)}}\right\} & f > 1 \end{cases} \quad \forall l \in \mathcal{L}\backslash\{L\}, m \in \mathcal{M}_l, f \in \mathcal{F}$$

From the above equation, we know that $\mathrm{t}^+_{i_f n_f\ lp} - \mathrm{t}^+_{i_f n_f\ lm} = t^*_{i_1 n_1\ lp} - t^*_{i_1 n_1\ lm}$, $\forall l \in \mathcal{L}\backslash\{L\}, m, p \in \mathcal{G}_{lk}$, $f \in \mathcal{F}$, only if no preceding AV departs at its earliest departure time. Please note that if an AV departs at its earliest departure time, the travel time delay cost of its following AVs would be the same at both nodes. Let denote the first AV in set $\mathcal{F}$ that departs at its earliest departure time (if it happens) by F^*. It is easy to show $n_{F^*} \geq N^*_{i_{(F^*)}}$. With this, we formulate the difference between the travel time delay costs of all preceding AVs of F^* at nodes $(l \in \mathcal{L}\backslash\{L\}, k \in \mathcal{K}_l, m \in \mathcal{G}_{lk})$ and $(l \in \mathcal{L}\backslash\{L\}, k \in \mathcal{K}_l, p \in \mathcal{G}_{lk})$ as follows.

$$\delta C^{\mathcal{F}}_{lpm} = \left(t^*_{i_1 n_1\ lp} - t^*_{i_1 n_1\ lm}\right). \sum_{f \in \{1, \dots, F^* - 1\}} \left(u_{i_f n_f}\right)$$

We know that the first CAV in set $\mathcal{F}$ is one the first AVs from one of the approaches. We also know that $t^*_{i(R_{lmi}+1)lm} \leq t^*_{i(R_{lpi}+1)lp}$, $\forall i \in \mathcal{I}$. With this, it is easy to show that $\left(t^*_{i_1 n_1\ lp} - t^*_{i_1 n_1\ lm}\right) = \left(t^*_{i(R_{lpi}+1)lp} - t^*_{i(R_{lmi}+1)lm}\right) \geq 0$. Since $n_{F^*} \geq N^*_{i_{(F^*)}}$, the above equation contains the travel time delay cost of at least all preceding AVs of $N^*_{i_{(F^*)}}$ from approach $i_{(F^*)} \in \mathcal{I}$. Thus, we can show that $\delta C^{\mathcal{F}}_{lpm} \geq \Delta C_{lpmi_{(F^*)}}$. This implies that if $C^{PV}_{lm} \leq C^{PV}_{lp} + \Delta C_{lpmi}$, $\forall i \in \mathcal{I}$, then for any feasible sequence of AVs (defined as the set $\mathcal{F}$) $C^{PV}_{lm} \leq C^{PV}_{lp} + \delta C^{\mathcal{F}}_{lpm}$. This conclude that node $(l \in \mathcal{L}\backslash\{L\}, k \in \mathcal{K}_l, p \in \mathcal{G}_{lk})$ is dominated by node $(l \in \mathcal{L}\backslash\{L\}, k \in \mathcal{K}_l, m \in \mathcal{G}_{lk})$ and can be pruned from the B&B tree. This completes the proof.

Proposition 4 indicates that there might be some branches in the B&B tree dominating other branches at the same level. This property of the problem helps the B&B algorithm to find the optimum solution in a more efficient manner. Although the number of dominated branches in the B&B tree depends on the parameter settings, it can be shown that the proposed valid cuts can improve the computational time complexity of the B&B algorithm from an exponential size to a polynomial size of the number of CAVs in a fully saturated traffic scenario i.e., $a_{in} = d_{in}$, $\forall i \in \mathcal{I}, n \in \mathcal{N}_i$. The following proposition specifies this property.

Proposition 5. The time complexity of the B&B algorithm with the proposed valid cuts in a fully saturated traffic scenario, where $a_{in} = d_{in}, \forall i \in \mathcal{I}, n \in \mathcal{N}_i$ and $N = \max_{i \in \mathcal{I}}\{N_i\}$ is $\mathcal{O}\left(N^{(I+1)}.I^3\right)$.

Proof. In the fully saturated traffic scenario where $a_{in} = d_{in}, \forall i \in \mathcal{I}, n \in \mathcal{N}_i$, the last PV's scheduled departure time at a node (l,m), i.e., $t^{+}_{(J_{lm})\left(R_{lm(J_{lm})}\right)}$, can be easily calculated by adding the summation of all PVs' minimum time headways to the summation of the total clearance time and the first PV's scheduled departure time. This basically indicates that two nodes in the same subset $\mathcal{G}_{lk}$ with the same number of switching approaches and the first and last PVs' approach indexes have the same scheduled departure time for the last PV. Hence, from Proposition 4, we know that there is one node dominating the other nodes with the same characteristics mentioned above. Now we know that there are no more than $\mathcal{O}(N^I)$ options for choosing a different number of CAVs from different approaches as PVs. For each of these options, there are no more than $\mathcal{O}(I.N)$ choices for the number of switching time headways. Further, for each of these options, there are at most $\mathcal{O}(I^2)$ choices for the first and last PVs' approach indexes. Thus, the optimal solution to the VSO problem in a fully saturated traffic scenario can be found by searching no more than $N^{(I+1)}.I^3$ nodes in the B&B tree. This basically means that the complexity of the B&B algorithm with the proposed valid cuts in a fully saturated traffic scenario is $\mathcal{O}\left(N^{(I+1)}.I^3\right)$. This completes the proof.

With these, we formulate the B&B algorithm to solve the VSO problem at a general conflict area considering heterogeneous CAV time headways and values of time.

An Illustrative Example

This subsection presents the key aspects of the B&B algorithm with an illustrative example. In this example, we focus on a conflict area consisting of two approaches with two CAVs on each approach, as shown in Figure 4(a). Each node of the B&B tree is denoted by a pair (l,m) which presents the level and node's index at that level. At each node (l,m), a set of information i.e., R_{lmi}, $t^{*}_{i(R_{lmi}+1)lm}, \forall i \in \mathcal{I}$, C^{PV}_{lm}, $C^{AV}_{lmi}, \forall i \in \mathcal{I}$, LB_{lm}, and UB_{lm}, is provided. The value of times adopted in this example are intended to highlight the algorithm's robustness and its ability to handle different inputs effectively, emphasizing the algorithm's versatility across a wide range of inputs. Further, the unvisited nodes visited nodes, chosen nodes for branching, and pruned nodes are shown in Figure 4(b)–(f) with yellow, white, green, and red colors, respectively. With these, the algorithm starts from a node at level 0 where $R_{lmi} = 0, \forall i \in \mathcal{I}$ as shown in Figure 4(b). Figure 4(c) then shows the B&B tree after the first branching. After updating GLB and GUB, node $(1,2)$ is chosen for next branching as presented in Figure 4(d). Going through the same procedure, Figure 4(e) shows the B&B tree after branching node $(1,1)$. It can be seen in Figure 4(e) that $t^{*}_{i(R_{21i}+1)21} \leq t^{*}_{i(R_{24i}+1)24}$ and $C^{PV}_{21} + C^{AV}_{21i} \leq C^{PV}_{24} + C^{AV}_{24i}, \forall i \in \mathcal{I}$. Hence, node $(2,4)$ is dominated by node $(2,1)$ based on Proposition 4 and is removed from the B&B tree. Finally, according to Figure 4(f), the B&B algorithm considering the valid cuts obtains the optimal solution after seven iterations, which is decreased by one compared to the B&B algorithm without considering the valid cuts.

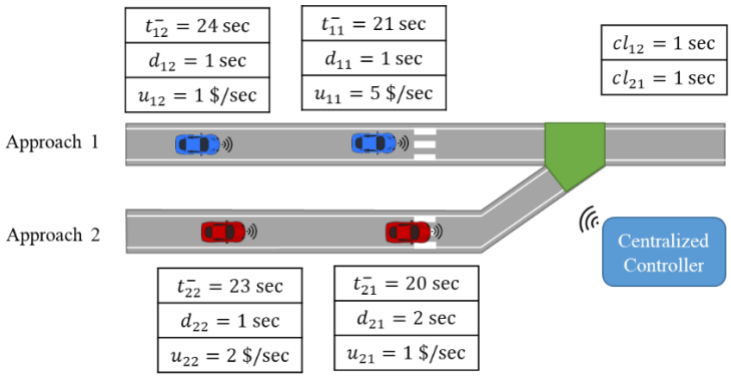

(a) An illustration to the example's parameter settings

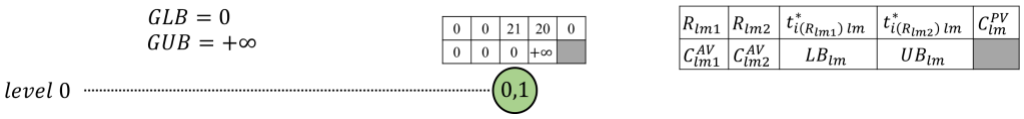

(b) Initial node of the B&B tree

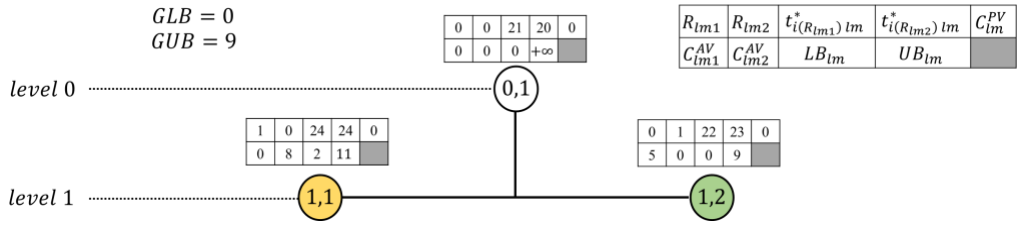

(c) The B&B tree after the first branching

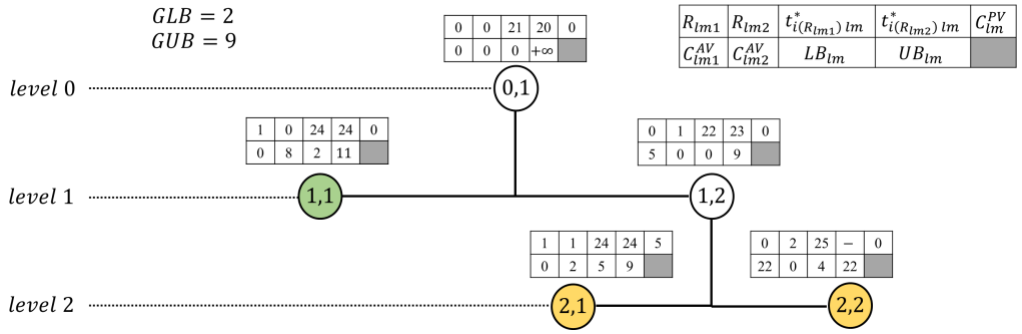

(d) The B&B tree after the second branching

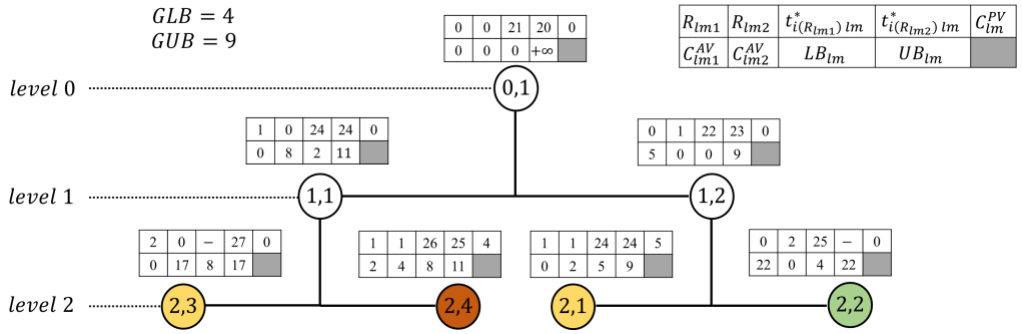

(e) The B&B tree after the third branching

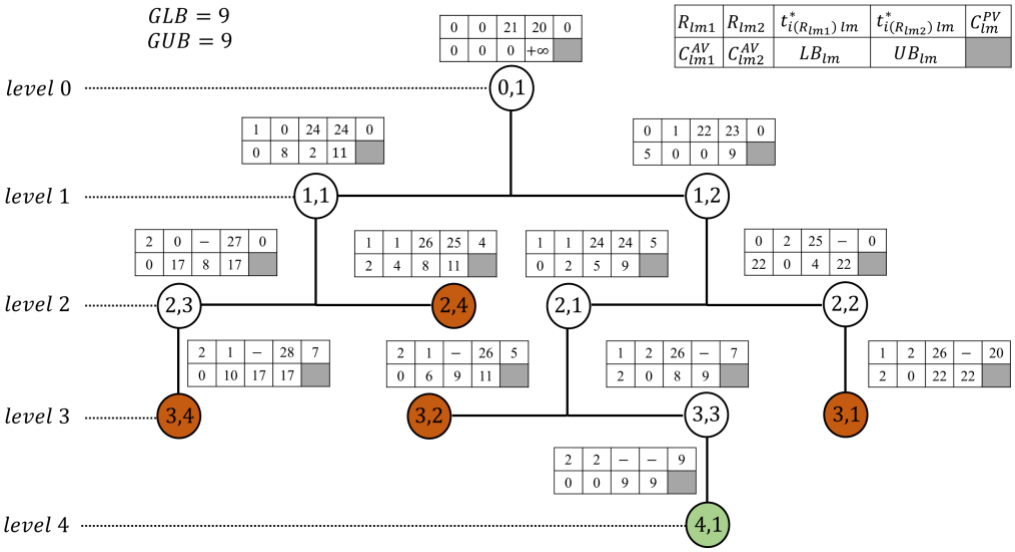

(f) The final B&B tree

Figure 4. An illustrative example of the B&B algorithm with the valid cuts.

Chapter 5. Numerical Experiments

This research presents a set of numerical experiments to investigate the performance of the proposed model and algorithm and illustrate the application of IVC. First, a set of numerical experiments in a fixed time horizon are conducted to investigate the computational complexity and accuracy of the proposed solution method. The second set of experiments further investigates the benefits of the IVC strategy compared to the outcomes of two benchmark cases for an isolated conflict area in a real-time application. Finally, sensitivity analysis is performed to draw managerial insights into the impacts of varying parameter settings such as lost time duration, length of control area, arrival traffic demand, heterogeneity in CAVs' value of time and minimum time headway on the proposed model's outcome. All numerical experiments were conducted on a DELL Studio PC with 3.60 GHz of Intel Core i7-7700 CPU and 16 GB RAM in a Windows environment and the proposed algorithm was implemented with Visual C++ 2017.

Fixed Time Horizon Experiments

This experiment considers an isolated conflict area consisting of two and three one-lane approaches with heterogeneous CAV time headways and values of the time. It basically means that each individual CAV can have different parameter settings. Thus, the parameter settings related to each individual CAV are randomly generated following a uniform distribution within their corresponding ranges. The maximum speed limits of all approaches are considered to be the same and equal to 30 meters/sec.

The value of time ranges from 1 to 10 is chosen to encompass a realistic and reasonable range commonly observed in transportation studies. This range allows for a comprehensive evaluation of the algorithm's performance across various value scenarios. By including a range of values, we capture the diversity in individuals' preferences and perceptions of travel time. This approach ensures a nuanced assessment of the algorithm's effectiveness and its applicability in real-world transportation planning and decision-making processes. Table 3 summarizes the default values of all parameters.

Table 3. Default Parameter Settings of CAVs

Parameter	Value	Note
a_{in}	$\in [1.2, 3]$ sec	$\bar{t_{i1}}, \forall i \in \mathcal{I}$,is assigned to an initial random number
u_{in}	$\in [1, 2, 3, 4, 5, 6, 7, 8, 9, 10]$ \$/sec	$\sim\lceil U(0,10)\rceil$
s_{in}	$\in [6, 12]$ meter	$\sim U(6,12)$
τ_{in}	$\in [0.4, 0.8]$ sec	$\sim U(0.4,0.8)$
cl_{ij}	$\in [0.6, 1.2]$ sec	$\sim U(0.6,1.2)$
$\bar{v}_i$	30 meter/sec	

Computation Performances of the Proposed Approaches

This subsection analyzes the computational performance and accuracy of the proposed solution method and control strategy. Different instances with various numbers of CAVs (5, 10, 15, 20, 25, 30) are tested to explore how the problem scale affects the B&B algorithm's computational performance. In these experiments, the computational time of the B&B algorithm is benchmarked against a state-of-the-art commercial solver, Gurobi. To explore whether the valid cuts presented in the B&B algorithm can improve the computational speed, we solve all instances with and without adding the valid cuts in the B&B procedure. To validate the effectiveness of the IVC strategy, a reservation-based control scenario (RBC) and a fixed-time signal control (FTSC) strategy are presented as benchmarks for all instances. In RBC, the passing sequence of CAVs is assumed to be in the first-in-first-out order. In FTSC strategy, the optimal cycle length is obtained through an enumeration procedure. For a given cycle length, the green splits for all directions are allocated in a way to produce equal degree of saturation on each approach (Gradinescu et al., 2007), which is formulated as follows.

$$G_i = (C - L).\frac{\overline{u}_i.\frac{\lambda_i}{\mu_i}}{\sum_{i\in\mathcal{I}} \overline{u}_i.\frac{\lambda_i}{\mu_i}}, \forall i \in \mathcal{I}$$

where G_i is the green time for each direction $i \in \mathcal{I}$, C is the cycle duration, L is the total clearance time of one cycle, $\frac{\lambda_i}{\mu_i}$ is the "volume per saturation flow" ratio for direction $i \in \mathcal{I}$, and $\overline{u}_i$ is the average priority of all CAVs in approach $i \in \mathcal{I}$. The values of λ_i, μ_i, $\overline{u}_i$, $\forall i \in \mathcal{I}$, and L are calculated with the following equations.

$$\lambda_i = \frac{N_i - 1}{\sum_{n\in\mathcal{N}_i\setminus\{1\}}(a_{in})} * 3600, \forall i \in \mathcal{I}$$

$$\mu_i = \frac{N_i - 1}{\sum_{n\in\mathcal{N}_i\setminus\{1\}}(d_{in})} * 3600, \forall i \in \mathcal{I}$$

$$\overline{u}_i = \frac{\sum_{n\in\mathcal{N}_i}(u_{in})}{N_i}, \forall i \in \mathcal{I}$$

$$L = \frac{\sum_{i\in\mathcal{I}}\sum_{j\in\mathcal{I}}(cl_{ij})}{I},$$

Then, a branch-and-bound algorithm is constructed to determine the optimal sequence of all phases within a cycle. Since the cycle length is fixed in FTSC, all phases should appear within a cycle duration, and also, no phase can appear consecutively moving from one cycle to another. Whit these, each instance of CAVs is solved with five approaches: individual-vehicle-based scenario using Gurobi (GB), individual-vehicle-based scenario using the B&B algorithm without the valid cuts (B&B_NV), individual-vehicle-based scenario using the B&B algorithm with the valid cuts (B&B_V), the analytical solution of reservation-based control (RBC) scenario, and the fixed-time signal control strategy (FTSC). Further, the time limit is set as five minutes for the first three solution approaches (i.e., GB, B&B_NV, and B&B_V). The outputs of all solution methods and their computational times are summarized in Table 4 and Table 5, respectively. Note that RBC and FTSC strategies are conducted as benchmarks only for the outputs of

the proposed model. Thus, no time limit for these two solution approaches is needed, and their computational times are not provided in Table 5.

Table 4. Statistics of Solution Quality Metrics - Numbers in Brackets Show Corresponding Gaps in Percentage

Number of approaches	Number of CAVs	Objective value ($) (Gap (%))				
		GB	B&B_NV	B&B_V	RBC	FTSC
2	5	76.4 (0)	76.4 (0)	76.4 (0)	179.2 (/)	132.5 (/)
	10	206.6 (0)	206.6 (0)	206.6 (0)	631.7 (/)	396.6 (/)
	15	313.6 (0)	313.6 (0)	313.6 (0)	1190.6 (/)	633.4 (/)
	20	450.4 (0)	450.4 (13.8)	450.4 (0)	2189.3 (/)	943.5 (/)
	25	573.6 (0.4)	586.1 (33.4)	573.6 (0)	3217.7 (/)	1253.8 (/)
	30	792.1 (1.6)	811.4 (51.7)	756.7 (0)	4986.2 (/)	1604.0 (/)
3	5	269.8 (0)	269.8 (0)	269.8 (0)	662.8 (/)	359.2 (/)
	10	1096.1 (10.6)	998.8 (43.8)	984.7 (0)	2375.9 (/)	1362.0 (/)
	15	2023.2 (14.8)	1874.4 (74.4)	1864.8 (0)	5072.9 (/)	2637.8 (/)
	20	3979.4 (18.8)	3304.0 (83.6)	3197.2 (0)	9680.9 (/)	4603.9 (/)
	25	5865.5 (21.4)	4679.0 (87.4)	4490.9 (0)	13784.4 (/)	6215.6 (/)
	30	8426.2 (23.2)	6582.6 (90.6)	6055.1 (35.8)	19888.5 (/)	8643.4 (/)

As shown in Table 4, GB, B&B_NV, and B&B_V provide exactly the same total travel time delay cost if they solve the problem optimally in the given time limit. This not only verifies the correctness of the proposed B&B algorithm but also indicates that the proposed cutting procedure in B&B is valid and does not compromise solution optimality. Table 4 also shows that B&B_V provides better solutions in terms of total travel time delay costs with smaller optimality gaps compared to all other solution methods. This verifies the effectiveness of the proposed valid cuts in the B&B procedure. Further, the RBC scenario produces significantly higher travel time delay costs compared to other control strategies, especially when their optimality gaps are zero. This also validates the effectiveness of the proposed individual-vehicle-based control compared to the reservation-based control, where the passing order of CAVs depends on their arriving order to the control area. Finally, the FTSC strategy always produces higher total travel time delay costs compared to the individual-vehicle-based scenario. An interesting observation here is that B&B_NV produces significantly lower travel time delay costs compared to GB, RBC, and FTFC, even if it cannot solve the problem to optimality. This verifies the effectiveness of the proposed upper bound procedure in the B&B algorithm and indicates that even the approximation of the total travel time delay cost in the individual-vehicle-based scenario outperforms the other control strategies in a given conflict area.

Table 5. Statistics of Computational Time Metrics for First Three Solution Approaches

Number of approaches	Number of CAVs	Computational time (sec)		
		GB	B&B_NV	B&B_V
2	5	0.06	0.01	0.01
	10	0.49	0.22	0.02
	15	2.79	10.12	0.04
	20	54.77	>300.0	0.11
	25	>300.0	>300.0	0.21
	30	>300.0	>300.0	0.43
3	5	0.82	1.81	0.05
	10	>300.0	>300.0	2.22
	15	>300.0	>300.0	8.68
	20	>300.0	>300.0	39.01
	25	>300.0	>300.0	167.66
	30	>300.0	>300.0	>300.0

Table 5 summarizes the computational times of GB, B&B_NV, and B&B_V. It is shown that the solution time of GB increases significantly as the instance size increases: that is, GB cannot solve the problem to optimality when the number of CAVs on each approach goes beyond 20 at a two-approach conflict area and when it goes beyond 5 at a three-approach conflict area. The computational speed of B&B_NV follows a similar trend as the computational speed of GB except for a higher growth rate. This verifies the exponential increase in that solution space as the problem size increases. This also indicates that, without the proposed valid cuts, the B&B algorithm would fail when used in real-time applications. However, after adding the valid cuts to the B&B algorithm, the optimal solution can be obtained in a much more efficient manner due to the solution space reduction. It can be seen in Table 5 that almost all instances in the two-approach conflict area can be solved within a second, which demonstrates the applicability of B&B_V to real-time applications in an isolated conflict area with no more than two approaches. As the number of approaches increases, B&B_V dominates all other solution approaches in terms of both computational speed and travel time delay cost. Although as the number of approaches increases, B&B_V takes a longer solution time, it can still be used in real-time applications of scheduling CAVs at conflict areas with three (or even more) approaches considering a smaller length of the control area with a lower number of CAVs on each approach.

Validation of Solution Space Reduction

To investigate whether the proposed valid cuts in the B&B algorithm can improve the computational speed, we solve all instances with B&B_V and B&B_NV and store the number of created nodes at each level. Figure 5 plots out the numbers of created nodes in both cases as the level increases for three different instances with a two-approach conflict area and one instance with a three-approach conflict area. As shown in Figure 5, without the valid cuts, the number of created nodes increases significantly as the level (i.e., the number of PVs) increases. This explains why the optimality gap in BAB_NV is even worse than GB given the same time limit. However, after adding the valid cuts, the number of created nodes decreases remarkably. This indicates that the proposed valid cuts can significantly decrease the solution space of the problem and as a result, reduce the computational time of the algorithm. Further,

Figure 6 plots out the number of explored nodes before finding the optimal solution (or a near-optimum solution if the time limit is reached) in GB, BAB_V, and BAB_NV over the problem size (e.g., indicated as the total number of CAVs) considering a two-approach conflict area. It can be seen in Figure 6 that the solution time of GB and BAB_NV increases almost exponentially as the problem size increases. It is noteworthy to mention that GB and B&B_NV cannot solve the problem to optimality for more than 20 CAVs on each approach in a two-approach conflict area. Hence, the number of explored nodes in these two solution approaches do not increase exponentially for the instances with more than 20 CAVs on each approach. However, the number of explored nodes in BAB_V increases at a much slower rate compared to GB and BAB_NV. An interesting observation from this figure is that as the problem size increases, the difference in the increase rate of explored nodes in B&B_V and B&B_NV also becomes more salient. This indicates that B&B_V is more effective during the peak hours when the conflict area has to serve higher traffic demand. Also, the system can benefit more from CAV technology using B&B_V by providing a longer control area.

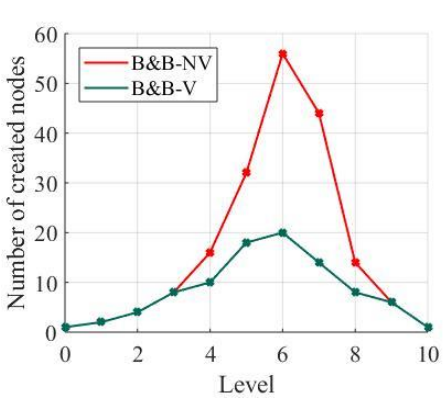

(a) Two-approach conflict area with 5 CAVs per approach

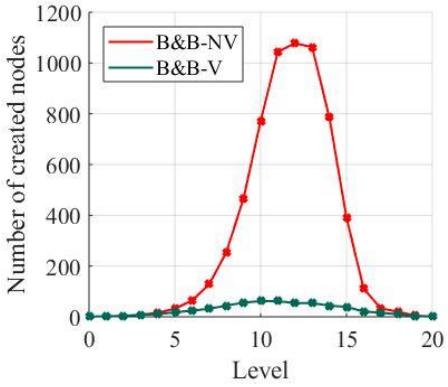

(b) Two-approach conflict area with 10 CAVs per approach

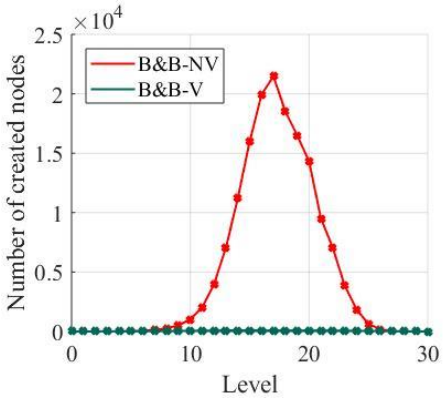

(c) Two-approach conflict area with 15 CAVs per approach

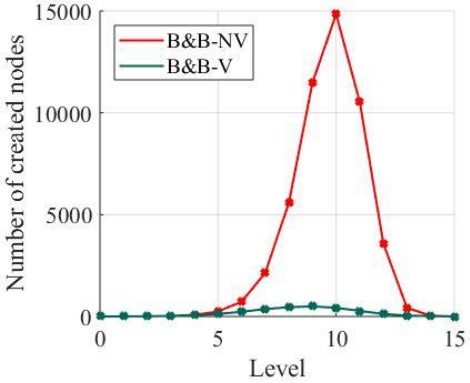

(d) Three-approach conflict area with 5 CAVs per approach

Figure 5. Number of constructed nodes in B&B tree before and after adding the valid cuts.

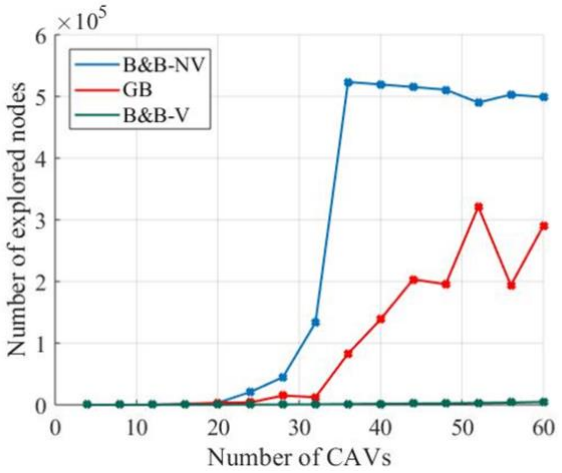

Figure 6. Number of explored nodes in Gurobi and B&B tree before and after adding the valid cuts.

Rolling Time Horizon Experiments

To monitor CAVs' operations while traveling within the control area, we use the analytical near-optimum trajectory construction method proposed by (Ghiasi et al., 2019). It basically restricts each CAV's trajectory to have no more than five quadratic segments (i.e., cruising, deceleration, stopping, acceleration, and cruising) with identical acceleration magnitudes to obtain smooth trajectories. In this experiment, we focus on isolated conflict areas consisting of two one-lane approaches, serving 1000 CAVs on each approach. The arrival traffic pattern on each approach is simulated by randomly generating each CAV's parameter setting. Two different patterns of arrival traffic demand rates are tested. As shown in Figure 7, we let the arrival traffic demand rates on each approach fluctuate to simulate both saturated and unsaturated traffic conditions. The fluctuation in the arrival traffic pattern is made consistent with a typical peak-hour cycle starting from unsaturated traffic, peaking at oversaturated traffic and finally ending at unsaturated traffic. This setting is to test the applicability of the proposed model to realistic time-varying traffic patterns.

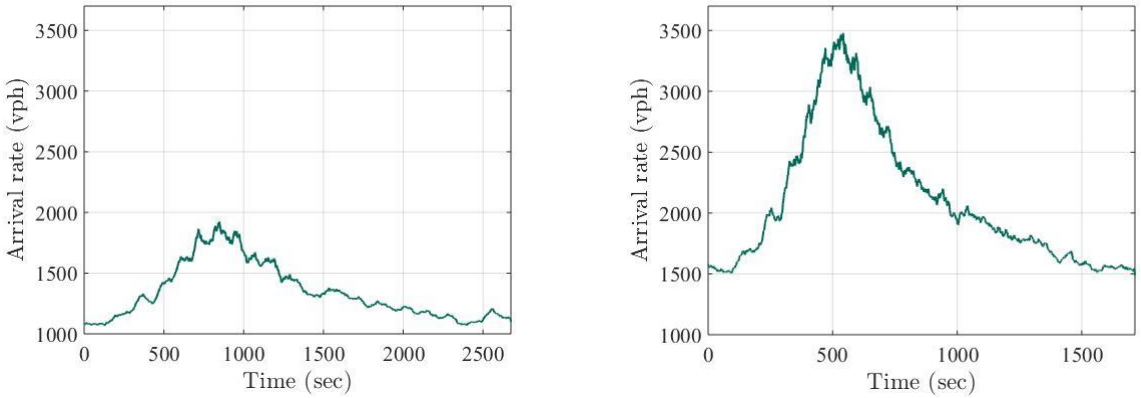

(a) Case I (b) Case II

Figure 7. Illustration of arrival traffic demand rate in a peak-hour cycle.

Table 6 summarizes the default values of all parameters related to the conflict area. Note that it is crucial to consider a maneuver area for each approach since CAVs must have enough space to adapt their movements given their scheduled departure times.

Table 6. Default Parameter Settings of Conflict Area

Parameter	Value	Note
$\bar{v}_i$	30 meter/sec	Free flow speed of approach $i, \forall i \in \mathcal{I}$
$\overline{a}_i$	4 meter/sec^2	Maximum safe acceleration rate on approach $i, \forall i \in \mathcal{I}$
$\underline{a}_i$	-4 meter/sec^2	Maximum safe deceleration rate on approach $i, \forall i \in \mathcal{I}$
l_i^m	1000 meter	Length of the maneuver area in approach $i, \forall i \in \mathcal{I}$
l_i^c	1000 meter	Length of the control area in approach $i, \forall i \in \mathcal{I}$

Further, Figure 8 illustrates the iterative procedure of conducting a rolling time horizon experiment in three steps. First, at a given scheduling time point, the set of CAVs located at the control area will be identified (green trajectories in Figure 8[b]). In the second step, the VSO problem will be constructed for this set of CAVs. Then, these CAVs will be scheduled to safely pass the conflict area using the B&B algorithm. Given the scheduled departure time of each set of CAVs, their trajectories will be constructed (blue trajectories in Figure 8[c]). Note that the scheduled CAVs might have a certain amount of travel time delay and as a result, the following set of CAVs may not be able to pass the conflict area without decreasing their speed. Thus, in the third step, the earliest departure time of the following set of CAVs will be updated after scheduling each set of CAVs (yellow trajectories in Figure 8[d]). We let the next set of CAVs to arrive the control area at the maximum speed to maximize the throughput of the conflict area. Further, in the third step, the earliest time an unscheduled CAV arrives to the end of the control area will be considered as the next scheduling time point. Going through this process iteratively, all CAVs from different approaches will be scheduled to safely pass the conflict area.

To evaluate the performance of the proposed solution method, the results of IVC are compared with the RBC and FTSC strategies. In RBC, we schedule CAVs in a first-in-first-out pattern at the second step of constructing rolling time horizon experiments presented for IVC. In the FTSC strategy, we obtain a near-optimum fixed-time cycle length for the whole horizon. The green splits of the signal setting is obtained with the same procedure described in the fixed-time horizon experiment. Note that CAVs are assumed to be smoothed in all three scenarios to ensure the fairness of the comparison. Therefore, CAVs in all three cases pass the intersection with maximum speed, which maximized the throughput and minimized the travel delay cost. This way, both RBC and FTSC scenarios are at their maximum performance level.

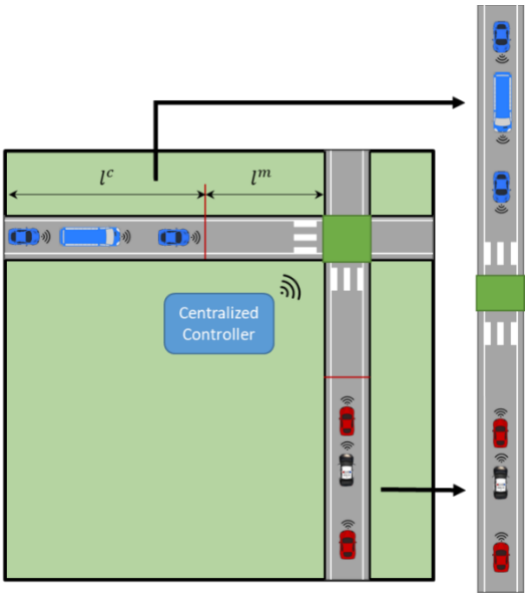

(a) An illustration to a two-approach conflict area

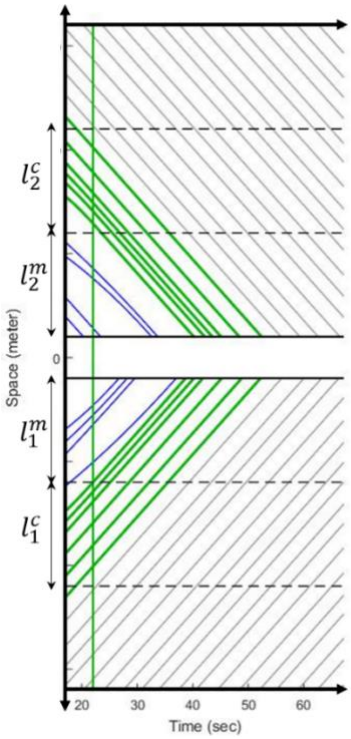

(b) Step 1 in constructing rolling time horizon experiment

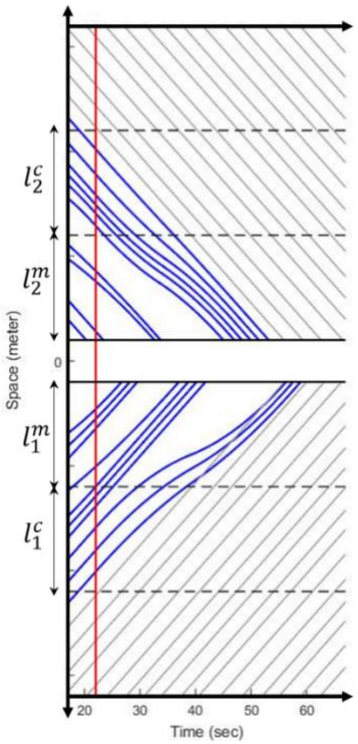

(c) Step 2 in constructing rolling time horizon experiment

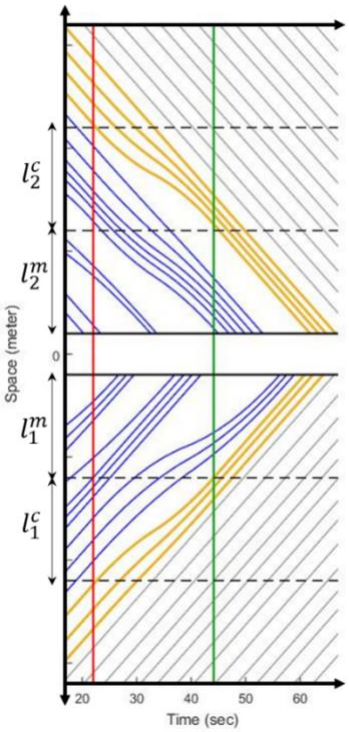

(d) Step 3 in constructing rolling time horizon experiment

Figure 8. Illustration of rolling time horizon experiment procedure.

To quantify the benefits, the results of all cases are compared on two measures: throughput at the conflict area and average travel time delay cost per CAV, denoted by Q and $\widehat{D}$, respectively. In all following experiments, $\widehat{D}$ is determined by dividing the total travel time delay cost to the total number of CAVs and Q is determined by dividing the total number of CAVs to the difference between the first and last CAVs' scheduled departure times.

Table 7 presents these measures for all cases. The results in Table 7 indicate that the proposed individual-vehicle-based control improves both measures compared to traditional reservation-based control (which can be used as a non-stop intersection instead of using stop signs) and fixed-time signal control (which can be found at many signalized intersections). These improvements are achieved by optimizing the departure sequence of CAVs at the intersection in real time. Optimizing the departure schedule aims to eliminate unnecessary delays by maximally using the shared space of the intersection box. Further, as shown in Table 7, the improvement in objective measures becomes more significant as the arrival travel demand increases. This shows that the proposed control strategy is more effective when the traffic is oversaturated.

Table 7. Rolling Time Horizon Simulation Quantitative Results

Demand Case	Scenarios	$\widehat{D}(\quad)$	Q(vph)
Case I	Individual-based control scenario (IVC)	1.6 (8.7)	2685.9
	Fixed time signal control scenario (FTSC)	4.0 (21.9)	2650.9
	Reservation-based control scenario (RBC)	256.8 (1399.8)	2342.0
Case II	Individual-based control scenario (IVC)	155.1 (845.2)	3832.5
	Fixed time signal control scenario (FTSC)	169.5 (923.7)	3306.4
	Reservation-based control scenario (RBC)	709.2 (3865.3)	2367.5

Sensitivity Analysis

A conflict area consisting of two approaches is considered for these sensitivity analyses. In all the experiments, we vary a specific input parameter while keeping the other parameters at their default values. To evaluate the system performance in these analyses, the same two measures used in the rolling time horizon experiments are considered: throughput at the conflict area (Q) and average travel time delay cost per CAV ($\widehat{D}$).

Figure 9 shows the results of the sensitivity analysis on clearance time duration $cl_{ij}, i, j \in \mathcal{I}, i \neq j$. In this sensitivity analysis, we assume that the clearance time between two approaches is the same (i.e, $cl_{12} = cl_{21}$) and for simplicity, we show this parameter value as cl in the figure. We let cl vary from 0 sec to 1.5 sec with the interval of 0.05 sec. As shown in Figure 9, the travel time delay cost per CAV increases almost linearly as the clearance time duration increases. Basically, the travel time delay cost of a CAV is highly affected by the extra delay time caused due to the additional clearance time. Further, we can see that the throughput of the conflict area has an inverse relationship with the clearance time. This observation is expected since increasing the clearance time duration consumes more time during the control operation.

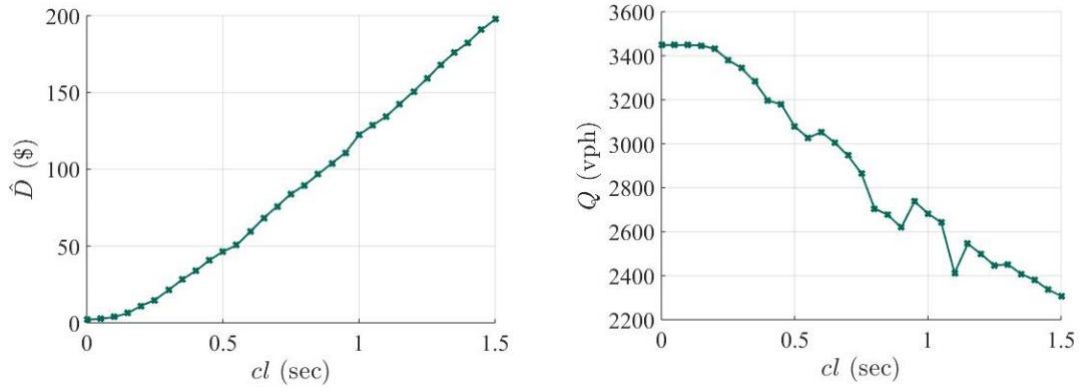

(a) (b)

Figure 9. Sensitivity analysis results on cl_{ij}, $i, j \in \mathcal{I}$, $i \neq j$.

Next, we conduct a sensitivity analysis on the length of the control area l_i^c, $i \in \mathcal{I}$ for the rolling-time horizon problem. In this sensitivity analysis also, we assume that the control area's length of both approaches are the same (i.e., $l_1^c = l_2^c$) and for simplicity, we show this parameter value as l^c in Figure 10. We let l^c vary from 200 m to 1600 m with an incremental interval of 100 m. It is noteworthy that in the rolling time horizon experiments, the whole arriving demand from an approach will be divided into different sets of CAVs. Then the VSO problem will be solved for each set of CAVs iteratively regardless of arriving demand at upstream. With this, it may not provide the true optimal solution of considering all CAVs at once. Hence, the operational measures in a rolling time horizon highly depend on the length of control area. As shown in Figure 10, increasing l^c results in lower travel time delay cost per CAV and higher throughput of the conflict area. In other words, identifying more CAVs at each scheduling time point can benefit the traffic system measures. However, there is a trade-off between the length of the control area and the computational time of finding an optimal sequence of CAVs. Thus, there might be a limitation on l^c due to high computational time required to solve a larger number of identified CAVs.

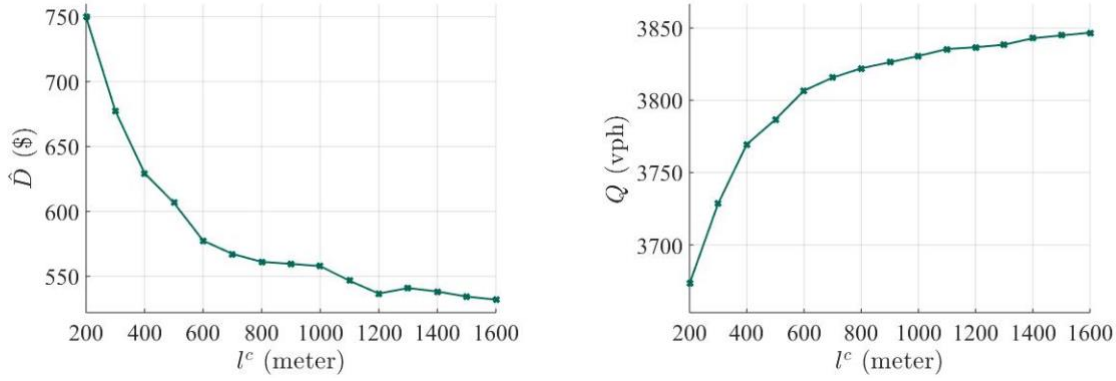

(a) (b)

Figure 10. Sensitivity analysis results on l_i^c, $i \in \mathcal{I}$.

Further, we perform a sensitivity analysis on the arrival traffic flow rate λ_i, $i \in \mathcal{I}$, and the results are shown in Figure 11. To simulate various arrival traffic flow rate λ_i, $i \in \mathcal{I}$, we first consider fully saturated scenario by setting the arrival headway of each two consecutive CAVs at each approach to the following

CAV's minimum time headway. Then, we decrease the arrival traffic flow rate iteratively by adding a random error term following uniform distribution between 0 sec and 0.1 sec to the arrival headway between every two consecutive CAVs. Going through this procedure 25 times for each approach, we simulate various arrival traffic flow rates. The sensitivity analysis results shown in Figure 11 indicate that both measures in general increase with λ_i, $i \in \mathcal{I}$. It is also shown that the computational complexity of the algorithm decreases with λ_i, $i \in \mathcal{I}$, which implies that the B&B algorithm improves the traffic performance more efficiently when the traffic demand on all approaches is close to the capacity.

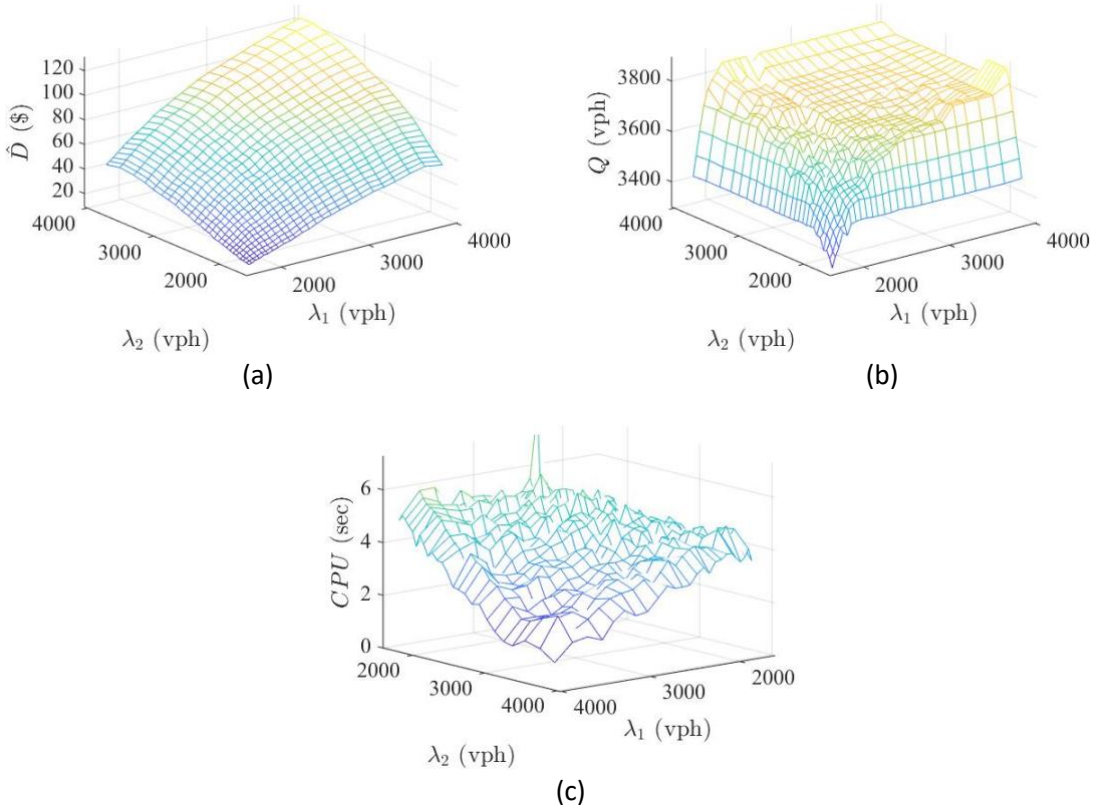

Figure 11. Sensitivity analysis results on λ_i, $i \in \mathcal{I}$.

Finally, to demonstrate how the heterogeneity assumption of the model affects the measures and complexity of the problem, a sensitivity analysis is performed on the heterogeneity of the minimum time headway and value of time. To simulate various scenarios of heterogeneous CAV priority, we let the maximum priority a CAV can have denoted by u^{max} vary from 1 \$/sec to 10 \$/sec with the incremental interval of 1 \$/sec. Note that each CAV must have a positive integer value as its priority. Thus, the minimum priority a CAV can have in all scenarios is 1 \$/sec. In the same way, to simulate various scenarios of heterogeneous CAV minimum time headway, we first set the minimum time headway of all CAVs as 1.2 sec. Then, we let the range of the randomly generated minimum time headway denoted by σ vary from 0 sec to 0.5 sec with the incremental interval of 0.02 sec. With these, we generate all CAVs priority and minimum time headway randomly following a uniform distribution within the given range at each iteration. The results of this sensitivity analysis are shown in Figure 12. As shown in this figure, $\hat{D}$ increases with u^{max} since the average priority of all CAVs increases as u^{max} increases. To have a fair comparison for different cases with various u^{max}, we also plot out the results

for travel time delay cost per priority unit denoted by D^u. It is shown that D^u only varies slightly across different u^{max} and σ. This indicates that the proposed IVC strategy can improve the total travel time delay cost even in a fully heterogeneous CAV environment. Next, we observe that considering heterogeneous CAV priority decreases the throughput of the conflict area while the heterogeneity in CAV minimum time headway has less impact on Q. This happens since the passing sequence of CAVs changes as we increase the variation of CAV priorities. Further, it can be seen from Figure 12 that heterogeneity in CAV minimum time headway and value of time complicate the VSO problem in terms of computational performance.

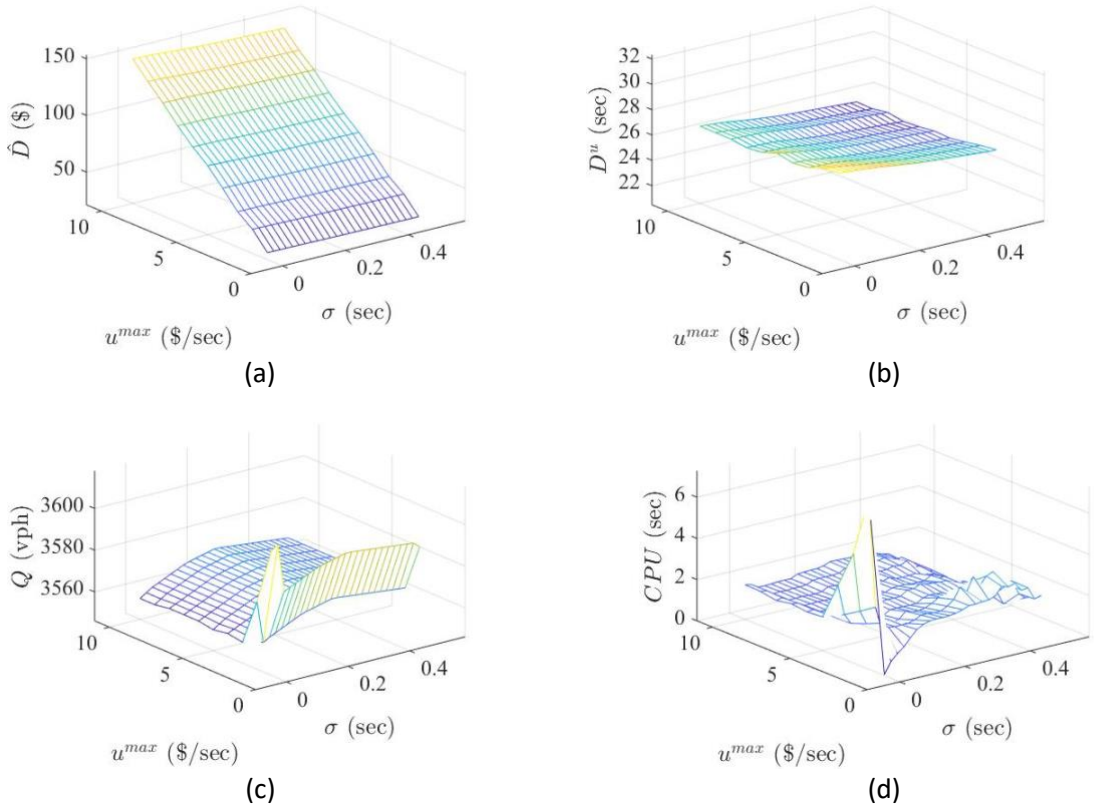

Figure 12. Sensitivity analysis results on u^{max} and σ.

Overall, these numerical experiments provide insightful information about the impact of different traffic conditions and roadway geometries on the model outcomes.

Chapter 6. Conclusion

This research proposed a practical TSP strategy at the single intersection level. A discrete modeling method is proposed to maximize intersection performance and give priority to transit. It gives out the exact optimal solution to the problem of vehicle scheduling at a general conflict area considering heterogeneous vehicle time headways and values of time in pure automated traffic.

This problem is formulated as a mixed-integer linear programming model that can be solved by state-of-the-art commercial solvers (e.g., Gurobi). The proposed problem is shown to be difficult to solve in an efficient manner since it is proven to be an NP-hard problem and its solution space increases exponentially as the problem instance size increases. To solve the problem in a more efficient manner, we propose a customized branch-and-bound algorithm to find the optimal sequence of CAVs passing the conflict area with the minimum total travel time delay cost. To increase the efficiency of the proposed algorithm, a set of valid cuts derived from the theoretical properties of the investigated problem is proposed and dramatically reduces the solution space of the investigated problem. Numerical experiments are performed to evaluate the proposed scheduling control strategy and the algorithm performance and to illustrate the application of this algorithm at a general conflict area. Further, the numerical analyses test the model on various traffic conditions and roadway geometries and investigate how the effectiveness of the proposed individual-vehicle-based control and branch-and-bound algorithm change with different input parameters. Overall, this study offers a methodological foundation to obtain the exact optimal solution to the real-world vehicle scheduling optimization problem at an isolated conflict area and provides meaningful insights into the various scheduling optimization problems accounting for different types of fleets, such as aircraft landing scheduling at a single runway, transit scheduling at the shared rail, and so on.

This study can be extended in a number of directions. First, though numerical experiments show that our customized branch-and-bound algorithm can solve the problem more efficiently compared to state-of-the-art commercial solvers, it would be interesting to investigate how parallel computing methods can enhance the solution efficiency. Further, while this study focuses on the scheduling problem in pure automated traffic environment, it will be worth investigating near-future scenarios with mixed traffic where only a portion of vehicles are CAV and the remaining vehicles are operated by human drivers. Also, while this study investigates the scheduling problem considering the fixed and equal arrival and departure speeds for all vehicles, it is interesting to investigate scenarios with heterogeneous arrival and departure speeds to account for more general traffic arrival patterns. For example, vehicles arriving to the conflict area from different approaches may need to satisfy different speed limits and they may head to different directions of the conflict area, which results in the different desired speed at the conflict area. The proposed model and algorithm can also be extended to account for conflict areas consisting of multi-lane approaches with more complex problem settings. It is also worth investigating how to scale up this concept to address scheduling problems of transits along a corridor or even across a network. Finally, investigating decentralized methods to schedule the transits and other vehicles at a general conflict area and comparing the results with the proposed centralized approach in this study is a potential future direction. Besides, deviations from the assumptions, such as significantly different vehicle speeds, complex maneuvering patterns, or control areas with varying lengths, may require further investigation and adaptations of the proposed method. Future research should focus on refining these assumptions and addressing their limitations to broaden the scope of our approach.

Several policy implications can be provided by this study. First, traveler delays can be a better optimization goal for signal control than vehicle delays, which further helps prioritize transits full of passengers. Potentially 12% extra people delay can be reduced with the traveler delay approach. This requires developing technologies to detect or track the number of travelers on each vehicle. Second, incorporating cutting-edge CAV technology into signal control is beneficial since it might lower energy consumption by 20% and increase capacity by 10%. Third, the collaboration between transit agencies and traffic management centers is needed to execute coordinated control.

References

Akcelik, Rahmi. Traffic signals: capacity and timing analysis. 1981.

Anderson, Paul, et al. “ScienceDirect E Ff Ect of Transit Signal Priority on Bus Service Reliability E Ff Ect of Transit Signal Priority on Bus Service Reliability.” Transportation Research Procedia, Vol. 38, Elsevier B.V., 2019, pp. 2–19, doi:10.1016/j.trpro.2019.05.002.

Au, Tsz-Chiu, and Peter Stone. "Motion Planning Algorithms for Autonomous Intersection Management." Bridging the gap between task and motion planning. 2010.

Campos, Gabriel R., et al. "Cooperative receding horizon conflict resolution at traffic intersections." 53rd IEEE Conference on Decision and Control. IEEE, 2014.

Cao, Wenjing, et al. "Cooperative vehicle path generation during merging using model predictive control with real-time optimization." Control Engineering Practice, 34 (2015): 98–105.

Ceylan, Halim, and Michael GH Bell. "Traffic signal timing optimisation based on genetic algorithm approach, including drivers’ routing." Transportation Research Part B: Methodological 38.4 (2004): 329–42.

Chanloha, Pitipong, et al. Cell Transmission Model-Based Multiagent Q-Learning for Network-Scale Signal Control With Transit Priority. No. 3, 2014, doi:10.1093/comjnl/bxt126.

Chow, Andy H. F., et al. “Multi-Objective Optimal Control Formulations for Bus Service Reliability with Traffic Signals.” Transportation Research Part B: Methodological, Vol. 103, 2017, pp. 248–68, doi:https://doi.org/10.1016/j.trb.2017.02.006.

Colombo, Alessandro, and Domitilla Del Vecchio. "Least restrictive supervisors for intersection collision avoidance: A scheduling approach." IEEE Transactions on Automatic Control, 60.6 (2015): 1515–27.

Daganzo, Carlos F., and Josh Pilachowski. “Reducing Bunching with Bus-to-Bus Cooperation.” Transportation Research Part B: Methodological, Vol. 45, No. 1, 2011, pp. 267–77, doi:https://doi.org/10.1016/j.trb.2010.06.005.

De La Fortelle, Arnaud. "Analysis of reservation algorithms for cooperative planning at intersections." 2010 13th International IEEE Conference on Intelligent Transportation Systems (ITSC). IEEE, 2010.

Dresner, Kurt, and Peter Stone. "A multiagent approach to autonomous intersection management." Journal of Artificial Intelligence Research, 31 (2008): 591–656.

Dresner, Kurt, and Peter Stone. "Multiagent traffic management: A reservation-based intersection control mechanism." Proceedings of the Third International Joint Conference on Autonomous Agents and Multiagent Systems, Vol. 2. IEEE Computer Society, 2004.

Ghiasi, Amir, et al. “A Joint Trajectory and Signal Optimization Model for Connected Automated Vehicles." No. 19-04445. 2019.

Gradinescu, Victor, et al. "Adaptive traffic lights using car-to-car communication." 2007 IEEE 65th Vehicular Technology Conference, VTC2007-Spring. IEEE, 2007.

Guler, S. I., Menendez, M., & Meier, L. (2014). Using connected vehicle technology to improve the efficiency of intersections. Transportation Research Part C: Emerging Technologies, 46, 121–31.

Hafner, Michael R., et al. "Cooperative collision avoidance at intersections: Algorithms and experiments." IEEE Transactions on Intelligent Transportation Systems 14.3 (2013): 1162–75.

Hu, Jia, et al. “Coordinated Transit Signal Priority Supporting Transit Progression under Connected Vehicle Technology.” Transportation Research Part C: Emerging Technologies, vol. 55, Elsevier Ltd, 2015, pp. 393–408, doi:10.1016/j.trc.2014.12.005.

Hu, Jia, et al. “Transit Signal Priority Accommodating Conflicting Requests under Connected Vehicles Technology.” Transportation Research Part C: Emerging Technologies, Vol. 69, 2016, pp. 173–92, doi:10.1016/j.trc.2016.06.001.

Huang, Shan, Adel W. Sadek, and Yunjie Zhao. "Assessing the mobility and environmental benefits of reservation-based intelligent intersections using an integrated simulator." IEEE Transactions on Intelligent Transportation Systems 13.3 (2012): 1201-1214.

Janos, Melanie, and Peter G. Furth. “Bus Priority with Highly Interruptible Traffic Signal Control: Simulation of San Juan’s Avenida Ponce de Leon.” Transportation Research Record, Vol. 1811, No. 1, SAGE Publications Inc, Jan. 2002, pp. 157–65, doi:10.3141/1811-19.

Jin, Qiu, et al. "Multi-agent intersection management for connected vehicles using an optimal scheduling approach." 2012 International Conference on Connected Vehicles and Expo (ICCVE). IEEE, 2012.

Kim, Kyoung-Dae, and Panganamala Ramana Kumar. "An MPC-based approach to provable system-wide safety and liveness of autonomous ground traffic." IEEE Transactions on Automatic Control 59.12 (2014): 3341–56.

Le, Tung, et al. "Decentralized signal control for urban road networks." Transportation Research Part C: Emerging Technologies 58 (2015): 431–450.

Lee, Joyoung, and Byungkyu Park. "Development and evaluation of a cooperative vehicle intersection control algorithm under the connected vehicles environment." IEEE Transactions on Intelligent Transportation Systems 13.1 (2012): 81–90.

Lee, Joyoung, et al. "Sustainability assessments of cooperative vehicle intersection control at an urban corridor." Transportation Research Part C: Emerging Technologies 32 (2013): 193–206.

Lenstra, Jan Karel, AHG Rinnooy Kan, and Peter Brucker. "Complexity of machine scheduling problems." Annals of discrete mathematics, Vol. 1. Elsevier, 1977. 343–62.

Levin, Michael W., and David Rey. "Conflict-point formulation of intersection control for autonomous vehicles." Transportation Research Part C: Emerging Technologies 85 (2017): 528–47.

Li, Zhuofei, et al. "Intersection Control Optimization for Automated Vehicles Using Genetic Algorithm." Journal of Transportation Engineering, Part A: Systems 144.12 (2018): 04018074.

Li, Zhuofei, Lily Elefteriadou, and Sanjay Ranka. "Signal control optimization for automated vehicles at isolated signalized intersections." Transportation Research Part C: Emerging Technologies 49 (2014): 1–18.

Liao, Chen-Fu, and Gary A. Davis. “Simulation Study of Bus Signal Priority Strategy: Taking Advantage of Global Positioning System, Automated Vehicle Location System, and Wireless Communications.” Transportation Research Record, Vol. 2034, No. 1, SAGE Publications Inc, Jan. 2007, pp. 82–91, doi:10.3141/2034-10.

Little, John D. C., et al. "An algorithm for the traveling salesman problem." Operations research 11.6 (1963): 972-989.

Lu, Xiao-Yun, and J. Karl Hedrick. "Longitudinal control algorithm for automated vehicle merging." International Journal of Control 76.2 (2003): 193–202.

Lu, Xiao-Yun, et al. "Automated vehicle merging maneuver implementation for AHS." Vehicle System Dynamics 41.2 (2004): 85–107.

Lu, Xiao-Yun, et al. "Implementation of longitudinal control algorithm for vehicle merging." Proc. 5th Int. Symp. Adv. Vehicle Control. 2000.

Ma, Wanjing, et al. “Development and Evaluation of a Coordinated and Conditional Bus Priority Approach.” Transportation Research Record, Vol. 2145, No. 1, SAGE Publications Inc, Jan. 2010, pp. 49–58, doi:10.3141/2145-06.

Makarem, Laleh, and Denis Gillet. "Model predictive coordination of autonomous vehicles crossing intersections." 16th International IEEE Conference on Intelligent Transportation Systems (ITSC 2013). IEEE, 2013.

Malikopoulos, Andreas A., Christos G. Cassandras, and Yue J. Zhang. "A decentralized energy-optimal control framework for connected automated vehicles at signal-free intersections." Automatica 93 (2018): 244–56.

Milanés, Vicente, et al. "Automated on-ramp merging system for congested traffic situations." IEEE Transactions on Intelligent Transportation Systems 12.2 (2011): 500–08.

Milanés, Vicente, et al. "Controller for urban intersections based on wireless communications and fuzzy logic." IEEE Transactions on Intelligent Transportation Systems 11.1 (2010): 243–48.

Milanés, Vicente, et al. "Cooperative maneuvering in close environments among cybercars and dual-mode cars." IEEE Transactions on Intelligent Transportation Systems 12.1 (2011): 15–24.

Mirchandani, Pitu, and Larry Head. "A real-time traffic signal control system: architecture, algorithms, and analysis." Transportation Research Part C: Emerging Technologies 9.6 (2001): 415–32.

Mirheli, Amir, Leila Hajibabai, and Ali Hajbabaie. "Development of a signal-head-free intersection control logic in a fully connected and autonomous vehicle environment." Transportation Research Part C: Emerging Technologies 92 (2018): 412–25.

Onieva, Enrique, et al. "Genetic optimization of a vehicle fuzzy decision system for intersections." Expert Systems with Applications 39.18 (2012): 13148–13157.

Pandit, K., Ghosal, D., Zhang, H. M., & Chuah, C. N. (2013). “Adaptive traffic signal control with vehicular ad hoc networks.” IEEE Transactions on Vehicular Technology, 62(4), 1459–71.

Pratt, Richard H., et al. Traveler Response to Transportation System Changes: Interim Handbook. 2000.

Qian, Xiangjun, et al. "Decentralized model predictive control for smooth coordination of automated vehicles at intersection." 2015 European Control Conference (ECC). IEEE, 2015.

Qian, Xiangjun, et al. "Priority-based coordination of autonomous and legacy vehicles at intersection." 17th International IEEE Conference on Intelligent Transportation Systems (ITSC). IEEE, 2014.

Rios-Torres, J., Malikopoulos, A., & Pisu, P. (2015, September). Online optimal control of connected vehicles for efficient traffic flow at merging roads. 2015 IEEE 18th International Conference on Intelligent Transportation Systems (ITSC), pp. 2432–37. IEEE.

Rios-Torres, Jackeline, and Andreas A. Malikopoulos. "A survey on the coordination of connected and automated vehicles at intersections and merging at highway on-ramps." IEEE Transactions on Intelligent Transportation Systems 18.5 (2017): 1066–77.

Robertson, Dennis I., and R. David Bretherton. "Optimizing networks of traffic signals in real time-the SCOOT method." IEEE Transactions on vehicular technology 40.1 (1991): 11–15.

Schrank, David, Bill Eisele, and Tim Lomax. "TTI’s 2012 urban mobility report." Texas A&M Transportation Institute. The Texas A&M University System 4 (2012).

Uno, Atsuya, Takeshi Sakaguchi, and Sadayuki Tsugawa. "A merging control algorithm based on inter-vehicle communication." Proceedings 199 IEEE/IEEJ/JSAI International Conference on Intelligent Transportation Systems (Cat. No. 99TH8383). IEEE, 1999.

Webster, Fo Vo. "Traffic signal settings." No. 39. 1958.

Wu, Jia, Abdeljalil Abbas-Turki, and Abdellah El Moudni. "Cooperative driving: an ant colony system for autonomous intersection management." Applied Intelligence 37.2 (2012): 207–22.

Wu, Jia, Abdeljalil Abbas-Turki, and Abdellah EL Moudni. "Intersection traffic control by a novel scheduling model." 2009 IEEE/INFORMS International Conference on Service Operations, Logistics and Informatics. IEEE, 2009.

Yan, Fei, Mahjoub Dridi, and A. E. Moudni. "A scheduling approach for autonomous vehicle sequencing problem at multi-intersections." International Journal of Operations Research 9.1 (2011).

Yan, Fei, Mahjoub Dridi, and Abdellah El Moudni. "An autonomous vehicle sequencing problem at intersections: A genetic algorithm approach." International Journal of Applied Mathematics and Computer Science 23.1 (2013): 183–200.

Yan, Fei, Mahjoub Dridi, and Abdellah El-Moudni. "New vehicle sequencing algorithms with vehicular infrastructure integration for an isolated intersection." Telecommunication Systems 50.4 (2012): 325–37.

Yang, Kaidi, S. Ilgin Guler, and Monica Menendez. "Isolated intersection control for various levels of vehicle technology: Conventional, connected, and automated vehicles." Transportation Research Part C: Emerging Technologies 72 (2016): 109–29.

Yin, Yafeng. "Robust optimal traffic signal timing." Transportation Research Part B: Methodological 42.10 (2008): 911–24.

Yu, Chunhui, et al. "Integrated optimization of traffic signals and vehicle trajectories at isolated urban intersections." Transportation Research Part B: Methodological 112 (2018): 89–112.

Zhang, Kailong, et al. "Analysis and modeled design of one state-driven autonomous passing-through algorithm for driverless vehicles at intersections." 2013 IEEE 16th International Conference on Computational Science and Engineering (CSE). IEEE, 2013.

Zhang, Yue, Andreas A. Malikopoulos, and Christos G. Cassandras. "Decentralized optimal control for connected automated vehicles at intersections including left and right turns." 2017 IEEE 56th Annual Conference on Decision and Control (CDC). IEEE, 2017.

Zhu, Feng, and Satish V. Ukkusuri. "A linear programming formulation for autonomous intersection control within a dynamic traffic assignment and connected vehicle environment." Transportation Research Part C: Emerging Technologies 55 (2015): 363–78.

Zou, Yun, and Qu, Xiaobo. "On the impact of connected automated vehicles in freeway work zones: a cooperative cellular automata model based approach." Journal of Intelligent and Connected Vehicles 1.1 (2018): 1–14.

NICR
NATIONAL INSTITUTE FOR CONGESTION REDUCTION

The National Institute for Congestion Reduction (NICR) will emerge as a national leader in providing multimodal congestion reduction strategies through real-world deployments that leverage advances in technology, big data science and innovative transportation options to optimize the efficiency and reliability of the transportation system for all users. Our efficient and effective delivery of an integrated research, education, workforce development and technology transfer program will be a model for the nation.

CUTR CENTER FOR URBAN TRANSPORTATION RESEARCH

Berkeley UNIVERSITY OF CALIFORNIA

Texas A&M Transportation Institute

UPR Recinto Universitario de Mayagüez

www.nicr.usf.edu